2011

The Role of the Propeptide and its Residues in Activation and Secretion of Elastase, an M4 Metalloprotease Secreted by Pseudomonas aeruginosa

Emily Boice

Virginia Commonwealth University

THE ROLE OF THE PROPEPTIDE AND ITS RESIDUES IN ACTIVATION AND SECRETION OF ELASTASE, AN M4 METALLOPROTEASE SECRETED FROM *PSEUDOMONAS AERUGINOSA*

A dissertation submitted in partial fulfillment of the requirements for the degree of Doctor of Philosophy at Virginia Commonwealth University.

by

EMILY NICOLE BOICE,
(B.S., Saint Louis University, 2005)

Director: Dennis E. Ohman,
Professor and Chair, Department of Microbiology and Immunology

Virginia Commonwealth University
Richmond, Virginia
May, 2011

ACKNOWLEDGEMENT

I would like to thank my mentor Dr. Dennis Ohman for his patience in answering all of my questions and for insightful discussions on my research projects. The vigorous training in the laboratory with designing and performing experiments, and interpreting results has helped prepare me for a future career in research. Dennis has continuously supported me throughout my graduate studies and has never hesitated to provide guidance when asked how I can improve on my work. His dedication to training students and encouragement of high quality work is greatly appreciated. Dennis has really inspired me to strive for excellence and I could not have been successful as a graduate student without his support.

I would like to thank my committee members, Dr. Jan F. Chlebowski, Dr. Cynthia N. Cornelissen, Dr. Walter M. Holmes, and Dr. Darrell Peterson, for their support and helpful suggestions on my research projects. I would also like to thank the former and current members of the lab for their support and valuable insight for my projects through discussions and presentations. I would especially like to thank Dr. Lynn Wood for the laughter, the help with experiments and crisis control. Lastly, I would like to thank my friends, family, and current and former colleagues for their continuous support and encouragement.

TABLE OF CONTENTS

LIST OF FIGURES

LIST OF TABLES

ABSTRACT

THE ROLE OF THE CONSERVED RESIDUES IN THE PROPEPTIDE OF ELASTASE SECRETED FROM PSEUDOMONAS AERUGINOSA

By Emily Nicole Boice, Ph.D.

A dissertation submitted in partial fulfillment of the requirements for the degree of Doctor of Philosophy at Virginia Commonwealth University.

Virginia Commonwealth University, 2011

Major Director: Dennis E. Ohman
Professor and Chair, Department of Microbiology and Immunology

Pseudomonas aeruginosa secretes several proteases associated with pathogenesis, but the most abundant and active is elastase (M4 metalloendopeptidase). Elastase (*lasB)*, is first synthesized as a preproenzyme, with a signal peptide, an 18-kDa N-terminal propeptide, and a 33-kDa mature domain. The propeptide functions as an intramolecular chaperone that is required for the folding and secretion of elastase, but ultimately is proteolytically removed and degraded. Previous research has identified the conserved residues in the propeptide of elastase as compared to other M4 protease precursors and showed some among them to be important for the production of active elastase. In this project, the ability of the propeptide alone to fold into a defined secondary structure was explored and a molecular model was created. Furthermore, the effects of substitutions on conserved residues in the propeptide of plasmid-encoded *lasB* pro alleles were assessed by expressing them in a *lasB* propeptide mutant. The kinetics of elastase activity in culture supernatants was quantitated using a fluorescent substrate, Abz-AGLA-p-Nitro-Benzyl-Amide, to provide an accurate assessment of the effects of mutant propeptides. *In*

vitro refolding studies were also performed to determine the effects of specific substitutions on foldase activity of the propeptide. When wild-type propeptide and mature elastase were denatured as separate proteins in guanidine-HCl buffer and renatured together, restoration of activity of the refolded elastase was measured, which was propeptide-dependent. Several mutant propeptides have now been shown to have defects using this *in vitro* foldase assay. Additional mutants were near wild-type activity level suggesting their role in recognition by the secretion apparatus. Residue locations were determined on a molecular model of the complex and confirmed the role of the secretion mutants as residues on the exterior. Residues that had diminished ability to refold in the *in vitro* assay were found to be in the interior parts of the complex, confirming their ability to be critical residues at the interface of the proteins or important in the stability of the propeptide's intrinsic structure. The goal was to perform a series of comprehensive analyses of the propeptide and its conserved residues in order to determine its role as an intramolecular chaperone.

INTRODUCTION

Pseudomonas aeruginosa infections

In January of 2009, *Pseudomonas aeruginosa* made international headlines in the medical community (Bradley Brooks, 2009). A beautiful young woman arrived in a Brazilian hospital in septic shock. Within two weeks, her feet and hands were amputated and she passed away days later. Mariana Bridi da Costa, a 20-year old Brazilian model and Miss World Finalist, had gone to the hospital right before the New Year complaining of kidney pain. She was quickly diagnosed with kidney stones and sent home. Within four days, her blood pressure had plummeted and her body went into septic shock. The *Pseudomonas aeruginosa* organism had entered her bloodstream and was quickly spreading through her body. In an effort to control the spread, her necrotic limbs were amputated but she succumbed to the infection in less than a month after the initial complaint.

Pseudomonas aeruginosa is a microorganism that exploits the human body to initiate a fatal infection. *P. aeruginosa* is a Gram-negative, aerobic bacillus of the Gammaproteobacteria class(Iglewski, 1996). This particular bacterium is the quintessential opportunistic pathogen of humans. It can infect nearly every tissue and system in the human body but rarely infects a healthy host. Furthermore, it is resistant to many antibiotics, and can mutate rapidly to become resistant to new drugs. This is a grave problem in patients that are hospitalized, particularly those with cancer, cystic fibrosis, and burns, where the noscomial infection fatality rate is 50%(Lyczak, Cannon, & Pier, 2000). In addition to these immune-compromised conditions, *P. aeruginosa* can cause a number of other diseases such as urinary tract infections, endocarditis, pneumonia, corneal infections, and ear infections.

Hospital-acquired infections are costly to the health-care system and a target of numerous strategies. This bacterium is particularly troublesome for hospitals because it is physically adaptive to diverse conditions. While its optimum growth temperature is 37°C, it is able to grow in lower and higher temperatures (Silo-Suh, Elmore, Ohman, & Suh, 2009). It is resistant to high salt concentrations and has very simple nutritional needs, requiring only acetate as a source of carbon and ammonium sulfate as a source of nitrogen. This organism can grow in soil and moist environments(Stratton, 1983) including hospital reservoirs: bottles of disinfectants, respiratory equipment, food, sinks, taps, toilets, showers and mops. It is constantly reintroduced into the hospital environment through fruits, plants, vegetables, as well by visitors and patients transferring from other facilities (Pitten, Panzig, Schroder, Tietze, & Kramer, 2001). Spread occurs from patient to patient through the hands of hospital personnel, by direct patient contact with contaminated reservoirs and by the ingestion of contaminated foods and water. The bacteria can form persistent biofilms. In its planktonic form it is free swimming, constantly looking for its next safe harbor (Jensen, Givskov, Bjarnsholt, & Moser, 2010). The spread of *P. aeruginosa* can best be controlled by observing proper isolation procedures, aseptic technique, and careful cleaning and monitoring of respirators, catheters, and other instruments (Pitten et al., 2001). Topical therapy of burn wounds with antibacterial agents such as silver sulfadiazine, coupled with surgical debridement, dramatically reduces the incidence of *P. aeruginosa* sepsis in burn patients(Shanmugasundaram, Uma, Ramyaa Lakshmi, & Babu, 2009).

Besides its ability to thrive in a number of hospital settings, *Pseudomonas aeruginosa* is notorious for its antibiotic resistance. The Gram-negative outer membrane affords the first level of antibiotic resistance to the organism. Additionally, its ability to form biofilms allows the species protection for its inner microcolonies, since the antibiotic would need to diffuse through

the extracellular matrix in order to affect the organisms (Davies & Bilton, 2009). *Pseudomonas* is able to maintain antibiotic resistance plasmids and transfer resistance genes by horizontal gene transfer via transduction and conjugation (Qiu, Kulasekara, & Lory, 2009). A limited number of antibiotics are successful against *Pseudomonas aeruginosa* (Wiener-Kronish & Pittet, 2011). These include fluoroquinolones, gentamicin, and imipenem but even these are not effective on all the strains. Several types of vaccines are being tested, but none are currently available for general use.

Diagnosis of *P. aeruginosa* infection depends upon isolation and laboratory identification of the bacterium. It grows well on most laboratory media and commonly is isolated on blood agar or eosin-methylthionine blue agar (Tielen et al., 2011). It is identified on the basis of its Gram stain morphology, inability to ferment lactose, a positive oxidase reaction, its fruity odor, and its ability to grow at 42°C (Tomlin, Coll, & Ceri, 2001). The colonies also fluoresce under ultraviolet light. This can be used to diagnose *P. aeruginosa* in wounds.

In addition to the ability of the organism to live in even the most harshest of environmental conditions, *P. aeruginosa* employs a number of virulence factors. A number of virulence factors (Figure 1) aid in adhesion. The bacterium has a single polar flagellum utilized for motility and dissemination (Conrad et al., 2011). The manner in which *P. aeruginosa* uses these virulence factors is resourceful. To first colonize, the organism needs the host to have a significant break in the first line of defense. This can include surgical trauma, tears and abrasions, or burns in the skin or mucosal areas (Pruitt, McManus, Kim, & Goodwin, 1998). Additionally, this can occur with the disruption of the normal human flora through the use of broad-spectrum antibiotics or a lapse in the immunologic defense mechanisms. Such a lapse can result from chemotherapy-induced neutropenia or the inability to clear mucus in the lungs of a

Figure 1. Virulence Factors of *Pseudomonas aeruginosa*

Classes	Mechanism of Action
Adhesins pili fimbriae alginate **Invasins** elastase lasA protease alkaline protease aminopeptidase hemolysins siderophores and siderophore uptake systems pyocyanin **Motility** flagella pili **Toxins** Exoenzyme S Exotoxin A Lipase	**Defense against serum bactericidal reaction** alginate, LPS, biofilm construction protease enzymes **Defense against immune responses** capsules, alginate, biofilm protease enzymes **Genetic attributes** genetic exchange by transduction and conjugation inherent drug resistance **Ecological criteria** adaptability to minimal nutritional requirements metabolic diversity widespread occurrence in a variety of habitats

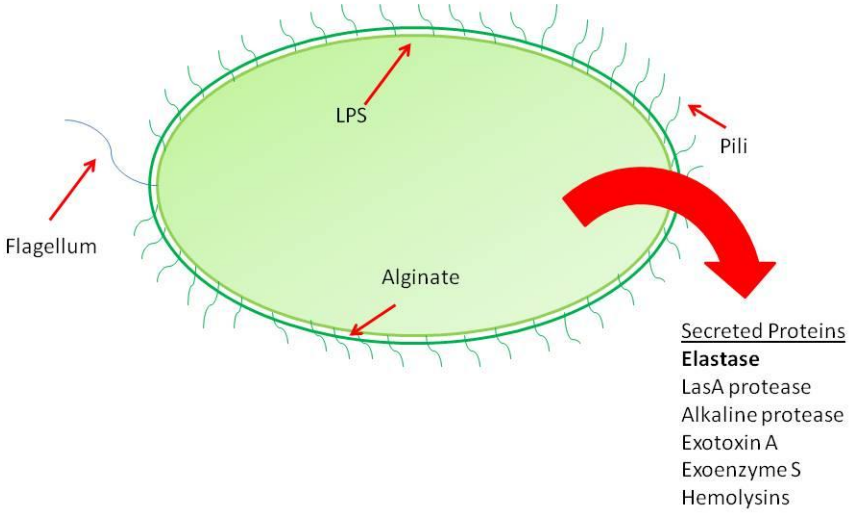

Figure 1. Virulence Factors of *Pseudomonas aeruginosa.*

(A) The virulence factors associated with the bacterium, *Pseudomonas aeruginosa.* They are classified by how the organism uses them to exploit the host to first colonize (adhesions), evade the host immune system (invasions), and move deeper into the host (motility and toxins). These individual virulence factors can play multiple roles in pathogenesis. Some of these are listed in the right-hand column.

(B) An illustration of the location of those some of the key virulence factors of *Pseudomonas aeruginosa.*

cystic fibrosis patient (Fujitani, Sun, Yu, & Weingarten, 2011). The first step in colonization is the "opportunisitic adherence" of the bacteria to compromised epithelium, typically using the bacteria's pili (Hertle, Mrsny, & Fitzgerald, 2001). The pili of *Pseudomonas aeruginosa* can adhere to the epithelial cells. The adhesins bind to specific galactose or mannose or sialic acid receptors on epithelial cells (Heiniger, Winther-Larsen, Pickles, Koomey, & Wolfgang, 2010). Colonization can also be aided by proteases which degrade fibronectin to further expose the pili receptor on the epithelial cell surface (Azghani, Kondepudi, & Johnson, 1992). After initial adhesion, pathogenesis can cause a chronic infection or an acute infection.

During a chronic lung infection seen in *P. aeruginosa* colonized patients with cystic fibrosis, the organism produces only low levels of non-cell associated virulence factors, such as toxins and proteases (Tingpej et al., 2007). This allows the bacteria to have sustainability in the host, using precious energy only to gather nutrients and build protective microcolonies (Mabrouk, Deffuant, Tolker-Nielsen, & Lobry, 2010). These microcolonies are protected further by the cell-associated virulence factors like alginate (Hay, Gatland, Campisano, Jordens, & Rehm, 2009), an exopolysaccharide that can aid in adhesion. Alginate allows for reduced clearance of the bacteria from the lung (Boucher, Yu, Mudd, & Deretic, 1997). It works to anchor the cells to their environment and, in medical situations, it protects the bacteria from the host defenses such as lymphocytes, phagocytes, the ciliary action of the respiratory tract, antibodies and complement (Song et al., 2003). The alginate allows for the *P. aeruginosa* infection to persist in the host for years.

However in acute infections, the ability of *Pseudomonas aeruginosa* to invade host tissues depends upon production of extracellular enzymes and toxins that break down physical barriers and damage host cells, as well as provide resistance to phagocytosis and the host immune

defenses (Adekoya & Sylte, 2009). Oftentimes, these acute infections can be introduced in the hospital setting. The introduction of bacteria into burn wounds is quite easy if non-sterile techniques are used. This can provide efficient bacterial colonization of the exposed, compromised epithelial tissues. The bacteria now use cell-to-cell signaling to amplify the extracellular virulence factors, such as toxins and proteases, to aid in dissemination (Parsek & Greenberg, 2000). These proteases can break down tissue integrity and inactivate host response molecules to allow the organism to migrate into the other tissues and the bloodstream.

This is however, a small view of the destructive capabilities of the organism. *Pseudomonas aeruginosa* can cause a number of other debilitating diseases. The organism infects heart valves of IV drug users as well as prosthetic heart valves by establishing itself on the endocardium by direct invasion from the blood stream(Reyes, Ali, Mendes, & Biedenbach, 2009). Respiratory infections caused by *Pseudomonas aeruginosa* occur almost exclusively in individuals with a compromised lower respiratory tract or a compromised systemic defense mechanism (Zemanick, Sagel, & Harris, 2011) . Primary pneumonia occurs in patients with chronic lung disease and congestive heart failure(Sun, Fujitani, Quintiliani, & Yu, 2011). Bacteremic pneumonia commonly occurs in neutropenic cancer patients undergoing chemotherapy (Fujita, Gu, Kishida, Okinaka, & Ohmagari, 2010). Lower respiratory tract colonization of cystic fibrosis patients by mucoid strains of *Pseudomonas aeruginosa* is quite common and difficult, if not impossible, to eradicate (Zemanick et al., 2011).

Pseudomonas aeruginosa can cause bacteremia primarily in immunocompromised patients and is acquired in hospitals and nursing homes (Fujimura, Nakano, Takane, Kikuchi, & Watanabe, 2011). Predisposing conditions include immunodeficiency resulting from AIDS, neutropenia, diabetes mellitus, and severe burns (Winsor et al., 2009).

This organism also causes meningitis and brain abscesses (Mena & Gerba, 2009). It invades the CNS from a nearby structure such as the inner ear or paranasal sinus (Suzuki, Nishiyama, Sugiyama, Miyamoto, & Baba, 1996). It can be inoculated directly by means of head trauma, surgery or invasive diagnostic procedures, or spreads from a distant site of infection such as the urinary tract (Chang et al., 2010).

Pseudomonas aeruginosa is the predominant bacterial pathogen in some cases of external otitis, including "swimmer's ear" (Reid & Porter, 1981). *Pseudomonas aeruginosa* can cause devastating infections in the human eye. It is one of the most common causes of bacterial keratitis (Stewart et al., 2011). *Pseudomonas* can colonize the ocular epithelium by means of a fimbrial attachment to sialic acid receptors (Wong, Sethu, Louafi, & Hossain, 2011). If the defenses of the environment are compromised in any way, the bacterium can proliferate rapidly through the production of enzymes such as elastase, alkaline protease and exotoxin A, and cause a rapidly destructive infection that can lead to loss of the entire eye (Twining, Kirschner, Mahnke, & Frank, 1993).

Urinary tract infections (UTI) caused by *Pseudomonas aeruginosa* are usually hospital-acquired and related to urinary tract catheterization, instrumentation or surgery. *Pseudomonas aeruginosa* is the third leading cause of hospital-acquired UTIs, accounting for about 12 percent of all infections of this type (Tielen et al., 2011). The bacterium appears to be among the most adherent of common urinary pathogens found in the bladder uroepithelium. In addition, *Pseudomonas* can invade the bloodstream through the urinary tract. Such infections account for nearly 40 percent of all *Pseudomonas* bacteremias infections (Shigemura et al., 2006), such as the patient in the introduction.

Pseudomonas aeruginosa can produce disease in any part of the gastrointestinal tract in immune-compromised individuals from the oropharynx to the rectum (Koh et al., 2010). It can also cause a variety of skin infections, both localized and diffuse. The common predisposing factors include a invasion of the integument which may result from burns, trauma or dermatitis; high moisture conditions such as those found in the ear of swimmers and the toe webs of athletes, hikers and combat troops, in the perineal region and under diapers of infants, and on the skin of whirlpool and hot tub users. *Pseudomonas* has also been implicated in folliculitis and unmanageable forms of acne vulgaris (Yu, Cheng, Wang, Dunne, & Bayliss, 2007).

Significance of *Pseudomonas* proteases

In a number of these disease types, bacterial proteases are often utilized in the organism's pathogenesis. *Pseudomonas aeruginosa* secretes several exoproteases, including elastase, lasA protease, and alkaline protease (Doring et al., 1987; Galloway, 1991). These are critical virulence factors, that work together to destroy tissue and damage host cell functions. Specifically elastase, an M4 metallopeptidase, has been shown to cleave the different components of tissue structure, including fibrin, collagen and elastin (El-Bazza, Moroz, Glatman, Samoilenko, & Terekhov, 1988), while it can also impair host proteases and defense mechanisms (Dulon et al., 2005). This protease is the most abundant extracellular endopeptidase secreted by *P. aeruginosa* and allows the bacteria to circulate further through the host (Kessler, E., and D. Ohman., 2004) .

Elastase: **Function and Utility**

Elastase is named for its ability to digest elastin (Kessler, E., and D. Ohman., 2004). Elastin is one of the most abundant components of almost every type of tissue, i.e., blood vessel

walls, lung, skin, and the bladder. It is a connective fiber with elastic properties which allow the tissue to retain its shape after contraction and expansion. Elastin also is primarily composed of four amino acids: glycine, valine, alanine, and proline. Elastin fibers are linked together to make a large, insoluble, resilient cross-linked array and this mesh is notoriously difficult to degrade (Heck, Morihara, & Abrahamson, 1986). Elastase is produced by over 80% of clinical isolates of P. aeruginosa (Wretlind, Heden, Sjoberg, & Wadstrom, 1973). Second to the ability to destroy elastin, elastase has the ability to degrade fibrin and collagen barriers as well as inactivate additional host proteins, including alpha-1-proteinase inhibitor, bronchial mucus proteinase inhibitor, lysozyme, complement components, IgG and IgA, along with inactivating signal inflammation cascades (Doring, Obernesser, & Botzenhart, 1981; Heck et al., 1990; Holder & Neely, 1989; Jacquot, Tournier, & Puchelle, 1985; Johnson, Carter-Hamm, & Dralle, 1982; Morihara, Tsuzuki, & Oda, 1979; Schultz & Miller, 1974). In addition to pulmonary tissue, corneal tissue, urinary tract, and vascular destruction have been linked to elastase activity (Gray & Kreger, 1975; Heck, Morihara, McRae, & Miller, 1986; Shigemura et al., 2006). Elastase works syngergistically with LasA protease (E. Kessler, Safrin, Olson, & Ohman, 1993), a serine protease that nicks the elastin and renders it susceptible to other enzymes like elastase. Most of the destructive tissue pathogenesis of *P. aeruginosa* can be attributed to these secreted enzymes (Wretlind & Pavlovskis, 1983).

Regulation of the production of many of the *Pseudomonas aeruginosa* virulence factors, including these enzymes, is tightly controlled by a mechanism which monitors bacterial cell density and provides communication between the bacteria by cell-to-cell signaling. Many gram-negative and gram-positive bacteria have developed the ability to sense their environmental conditions and populations through cell-to-cell signaling, also called quorum sensing(Parsek &

Greenberg, 2000). This enables the bacteria to secrete the virulence factors only at optimal times for the pathogenesis. The bacteria do this by producing a small molecule called an autoinducer (AI) which is free to diffuse through the cell membrane and away from the cell. In low density populations, the AI diffuses away from the cell into the media and becomes diluted. With increasing bacterial cell density, the concentration of this AI accumulates and reaches a threshold level. The small molecule is now able to bind a transcriptional activator protein, forming a complex which is able to bind DNA sequences upstream of target genes enhancing their transcription. In *Pseudomonas aeruginosa*, there are two circuit systems that interact to ensure the precise and abundant production of elastase (Pearson, Pesci, & Iglewski, 1997). The autoinducers responsible for elastase synthesis are 3-oxo-C12-HSL (N-[3-oxododecaolyl]-L-homoserine lactone) and C4-HSL (N-butyrylhomoserine lactone)(Passador, Cook, Gambello, Rust, & Iglewski, 1993; Passador et al., 1996). The AI synthase gene responsible for the first AI (3-oxo-C12-HSL), is *lasI* and the *lasR* gene codes for the transcriptional activator protein (Sappington, Dandekar, Oinuma, & Greenberg, 2011). Additionally, the *las* system has been shown to activate the genes necessary for the transport of these enzymes from the cell (Rust, Pesci, & Iglewski, 1996).

The organism has a backup mechanism in the second circuit, the *rhl* system(Wilder, Diggle, & Schuster, 2011). The second AI (C4-HSL) is encoded by the *rhlI*, the AI synthase gene, while the *rhlR* gene encodes the transcriptional activator protein (Netotea et al., 2009). This circuit has the ability to activate production of some of the same virulence factors but the preferred promoters are the *las* promoters.

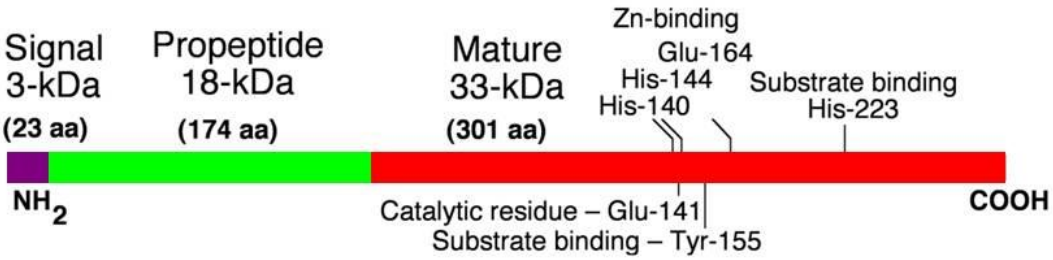
Signal
3-kDa
(23 aa)
Propeptide
18-kDa
(174 aa)
Mature
33-kDa
(301 aa)
Zn-binding
Glu-164
His-144
His-140
Substrate binding
His-223
NH2
Catalytic residue – Glu-141
Substrate binding – Tyr-155
COOH

Figure 2. The three domain polypeptide is illustrated. The purple domain is the pre domain (called the signal sequence), the green domain is the propeptide domain, and on the carboxyl end is the mature domain indicated in red. The residues highlighted on the mature domain (red) are those involved in the HEXXH motif (H140, E141, V142, S143, final H144), and additionally those needed for substrate binding (Y155 and H223). The catalytic residue E141.

System (Wilder et al., 2011). This intricate circuitry allows for the production of the virulence factors to be most beneficial for the organism.

Additionally, the bacteria have evolved another way to control the mechanism of action of elastase. Most prokaryotic proteases are synthesized as zymogens or inactive precursors (proenzymes) (Khan & James, 1998). Both LasA protease and elastase secreted are proenzymes by *P. aeruginosa* (E. Kessler, Safrin, Gustin, & Ohman, 1998). These zymogens are normally activated only after the polypeptide has been localized to its predestined site of action, which can be either intracellularly or extracellulary. Elastase is one of these zymogens and is encoded by *lasB* (*Pseudomonas aeruginosa* locus PA3742) (Stover et al., 2000; Winsor et al., 2009; Winsor et al., 2011). This gene is located between 4170483 – 4168987 Mbp on the genome of strain PAO1 and encodes a 498 amino acid (53.6-kDa) protein, called pre-proLasB (Bever & Iglewski, 1988; Fukushima et al., 1989). This larger precursor (Figure 2) is composed of a 2.6 kDa (23 residues) signal peptide that is followed by an 18 kDa (174 residues) propeptide and the 33 kDa mature domain (301 residues) (Bever & Iglewski, 1988). However, only a 33-kDa protein is found in the culture supernatant (Wolz et al., 1991). The aim of this project is to elucidate the role of the propeptide domain in folding and activating the mature domain.

Initially all three domains are synthesized within the cytoplasm (Figure 3). The signal peptide is removed upon secretion from the Sec system into the periplasm (Braun, Bitter, & Tommassen, 2000). Once within the periplasm, the propeptide is autocatalytically cleaved and forms a non-covalent complex with the mature domain. The mature domain also forms disulphide bonds within the periplasm (Braun et al., 2001). This complex is recognized by the Type II secretion system (T2SS) and secreted into the extracellular environment (Braun, Tommassen, & Filloux, 1996). T2SSs are complex machines consisting of 12–16 components,

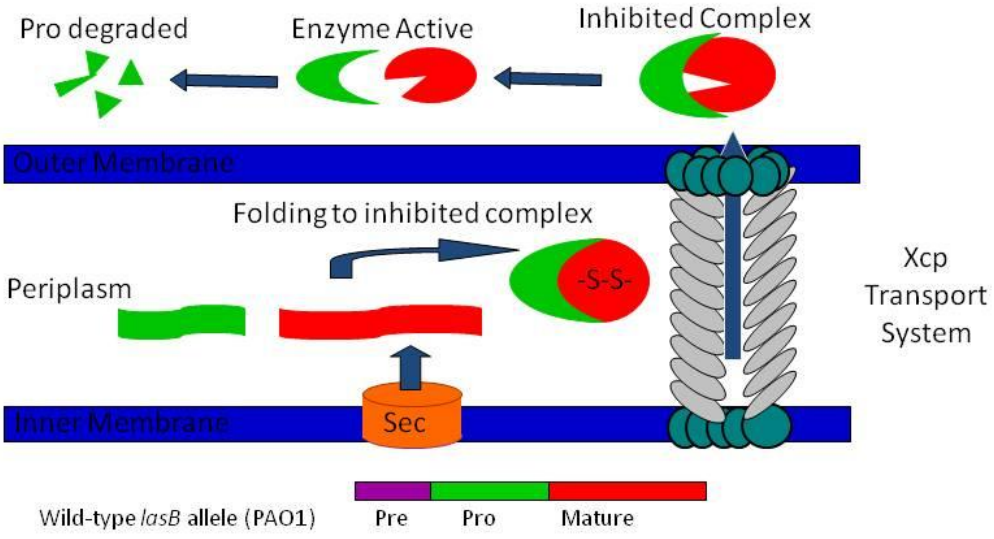
Pro degraded
Enzyme Active
Inhibited Complex
Outer Membrane
Folding to inhibited complex
-S-S-
Periplasm
Xcp
Transport
System
Inner Membrane
Sec
Wild-type lasB allele (PAO1)
Pre
Pro
Mature

Figure 3. The folding and secretion model of the zymogen known as Elastase. Within the bacterial cytoplasm, all three domains of the polypeptide are seen. The "pre" domain (signal sequence) is lost upon secretion into the periplasm via the Sec transport system. The propeptide domain and the mature domain within the periplasm are then autocatalytically cleaved and folded into an inhibited complex. Here the disulphide bonds also form in the mature domain. This inhibited complex is recognized by the Type II secretion system (Xcp transport system in *Pseudomonas*). The inhibited complex is then transported extracellularly and the propeptide domain dissociates from the mature domain. It is degraded by the now active elastase and other extracellular proteases.

which are generically named Gsp, or Xcp in the case of the main T2SS in *Pseudomonas aeruginosa* (Filloux, Michel, & Bally, 1998). The Xcp system of *P. aeruginosa* is important for the secretion of many different proteins, including elastase, lipase, phospholipases, chitin-binding protein and exotoxin A (Koster, Bitter, & Tommassen, 2000). The system is encoded by 12 *xcp* genes. Production of the system is regulated by quorum sensing and it has been estimated that 50–100 Xcp complexes are present in the cell at high cell densities (Russel, 1998).

Initially the complex is seen outside the cell. However, after a short period of time, the abundant protein is found to be the 33-kDa mature domain (E. Kessler & Safrin, 1994). Current research suggests that the propeptide appears to be critical for folding within the periplasm and secretion but not for the activity of the enzyme. This function proposes a need for understanding the propeptide-mediated folding of the mature domain and catalysis of the individual complex components which are both required for final enzyme activation.

Elastase: Structure

Elastase is a member of the M4 family of Thermolysin-like Neutral zinc-metallo Proteases (TNP). This protease has previously been termed Pseudolysin (EC 3.4.24.26), due to its 49% simillarity to Thermolysin, an M4 metalloprotease secreted by *Bacillus thermoproteolyticus* (Kessler, E., and D. Ohman., 2004). The crystal structure of the mature active enzyme has been solved to 1.5 angstrom resolution (Figure 4) (Thayer, Flaherty, & McKay, 1991). Both proteases, elastase and thermolysin, contain a single zinc atom essential for activity, observed by metal chelation experiments inhibiting enzymatic activity (E. Kessler, Israel, Landshman, Chechick, & Blumberg, 1982). The active site catalytic residue (Glu-141) for elastase has been determined along with the zinc coordination residues (His-142, His-146,

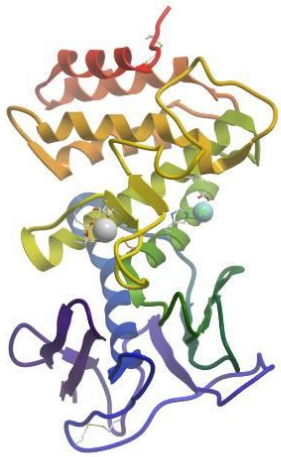

A

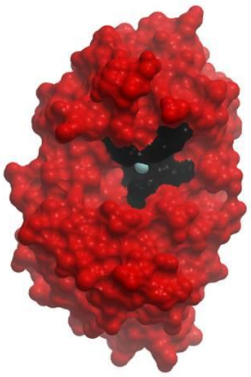

B

Figure 4. (A) Shown is a ribbon diagram of the crystal structure of the mature domain of elastase (PDB 1EZM) by Dr. McKay in published in 1991. The grey sphere in the middle right is the zinc ion, the left one is the calcium ion. The two globular regions are shown by the presence of alpha helices and the beta strands. The amino terminus of the enzyme is seen at the bottom of the structure (bottom – left, second beta sheet in). The carboxyl terminus is on the top (attached to the furthest red alpha helix).

(B) Shown is a space filling model of the enzyme. The residues in the substrate cleft are shown in black. The grey sphere is the coordinated zinc atom.

and Glu-166) (Kawamoto et al., 1993). Elastase also requires calcium ions for stabilization (Olson & Ohman, 1992). Additionally, substantial conformational differences were observed when the enzyme was either in the absence of ligand or in the presence of a covalent noncompetitive inhibitor as compared to tight-binding competitive inhibitors (McKay, Thayer, Flaherty, Pley, & Benvegnu, 1992). The first group maintains an "open" substrate binding cleft while competitive inhibitors allow the cleft to close.

Elastase favors certain residues for its substrate specificity. Hydrophobic or aromatic amino acid residues are optimal for the residue that is just to the carboxyl terminus of the substrate cleavage site (P1' position). The order of preference for residues at P1' is Phe >Leu >Tyr >Val >Ile. Aromatic residues seem to be preferred to aliphatic residues (Kessler, E., and D. Ohman., 2004). Ala is favored at the P1 (the residue at the position amino terminal to the substrate cleavage) and P2' (carboxy to the P1' residue) positions, and elongation of the substrate to the P2 and P2' positions results in a marked increase in the rate of hydrolysis (Kessler, E., and D. Ohman., 2004).

The family of M4 metalloproteases is classified based on a number of characteristics. According to the MEROPS peptidase database, elastase is a member of the MA clan of peptidases. The members of this clan have water bound by a single zinc ion which in turn is ligated to two His residues and Glu residue, and an additional His or Asp (Rawlings & Barrett, 1993). This clan contains a variety of metallopeptidases and all have the conserved HEXXH motif where the two His residues coordinate a zinc ion and the Glu has a catalytic function (Rawlings, Barrett, & Bateman, 2010). Elastase is further classified within the M4 family of the MA clan. Unique to the M4 family is the fact that the endopeptidases all bind a single zinc ion and use a Glu residue further towards the C-terminus of the HEXXH motif in the protein's

mature domain (Jongeneel, Bouvier, & Bairoch, 1989). The zinc ion is tetrahedrally co-ordinated and the fourth ligand is activated water, which forms the nucleophile in the catalysis reaction (Rawlings & Barrett, 1993). Most of the M4 family members are active at a neutral pH and degrade substrates with the preference of cleaving after hydrophobic residues and before Leu, Phe, Ile and Val (MEROPS). Of the 22 members identified in this family, five have been crystallized, (thermolysin PDB: 1NPC, vibriolysin PDB: 3NQX, elastase PDB: 1EZM, aureolysin PDB: 1BQB, and protealysin PDB: 2VQX)(Banbula et al., 1998; Demidyuk et al., 2010; Gao et al., 2010; Stark, Pauptit, Wilson, & Jansonius, 1992; Thayer et al., 1991). The mature genetic domains have a two globular domain structure with the active site between the structural domains. They have N-terminal propeptides that are autocatalytically removed upon secretion of the enzymes from the cells. However little is known about their propeptide domains. The propeptide of elastase has two folds, identified by sequence homology in the Pfam protein fold database: PepSY and FTP (Braun et al., 2000). The PepSY fold is likely to have a protease inhibitor function and the Fungalysin/Thermolysin Propeptide Motif fold (FTP) is likely to either inhibit the peptidase by preventing premature activation or acts as a chaperone for the mature domain.

Currently, we understand that the propeptide is secreted with the enzyme and processing of the mature domain is autocatalytic (McIver, Kessler, Olson, & Ohman, 1995). During this initial secretion time period, short-term *Pseudomonas aeruginosa* cultures showed that inactive elastase-propeptide complex is secreted from the cells (E. Kessler & Safrin, 1994). Immunoblots (Figure 5) of these washed cell cultures, to limit proteolysis, confirm the presence of the propeptide in the supernatant for up to one hour, followed by degradation (E. Kessler & Safrin, 1994). After the secretion of the complex occurs (by 60 minutes), the propeptide is degraded

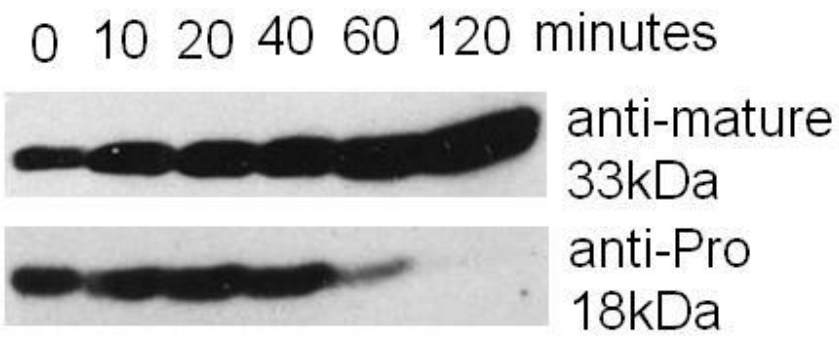
0 10 20 40 60 120 minutes
anti-mature
33kDa
anti-Pro
18kDa

Figure 5. Washed cell culture assays were used to identify the time frame propeptide seen in the supernatant of cultures, modified from (E. Kessler & Safrin, 1994). Cultures of *P. aeruginosa* were grown for 18 hrs and the cells were washed and resuspended in fresh media and protease inhibitors. Aliquots of the culture were taken at designated time points (shown in minutes) and spun. The supernatants were TCA precipitated and run on an SDS-PAGE and transferred. These immunoblots were probed with anti-Elastase antibodies (top panel) and anti-Propeptide antibodies (bottom panel). Propeptide was found for up to an hour after induction, as seen by the band in the bottom panel. Afterwards, it is degraded. This provides evidence that propeptide is required for secretion into the extracellular space.

extracellularly by elastase and other secreted active proteases (E. Kessler et al., 1998). Propeptide alone is not secreted from the cell (data not shown). *In vitro* zymogram experiments have shown the propeptide acting as an effective inhibitor of the protease (E. Kessler & Safrin, 1994). When elastase is mixed with increasing volumes of periplasmic fractions (which contain the propeptide), and run on a zymogram using skim milk as a substrate, the elastase loses its activity.

To further examine the interaction between the propeptide and elastase, studies were performed to overexpress the two components in *trans* in *E. coli* (McIver et al., 1995). While *E. coli* K12 cannot secrete the active enzyme past the outer membrane due to the lack of Xcp transport machinery, the propeptide-enzyme complex is autoprocessed to an active enzyme form (33-kDa) while remaining in the periplasm, confirming the propeptide processing from the enzyme is autocatalytic. A propeptide deletion allele (*lasB6*) was exchanged into the *Pseudomonas* chromosome and complemented with the propeptide expressed in *trans* (*lasB7*). This system (Figure 6) showed elastase activity measured outside the cell. When the *lasB6* allele, encoding a pre-mature segment without the propeptide, is expressed in *E. coli,* the enzyme product is inactive. Expression of this propeptide deleted allele also resulted in the accumulation of the inactive enzyme within the cell. The only way to restore activity of the enzyme was through co-expression of the *lasB7* allele encoding the pre-propeptide. Therefore the propeptide is needed in *cis* or in *trans* for the secretion of the mature enzyme as well as for its activation.

When specific amino acid residues on the mature domain, such as His-223 (substrate-binding residue) are changed to Asp (*lasB1*) or Tyr (*lasB2*) in order to block proteolytic activity, the 51-kDa precursor accumulates in the cell with the signal peptide removed, associating with

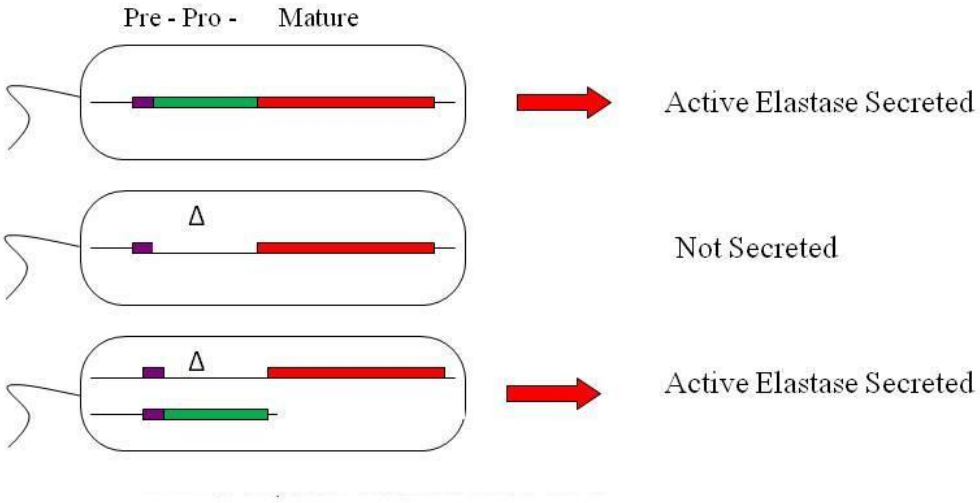
Pre - Pro -
Mature
Active Elastase Secreted
Δ
Not Secreted
Δ
Active Elastase Secreted

Figure 6. The propeptide has been shown to interact with the mature domain in *cis* and in *trans*. Experiments examined the presence and absence of the propeptide domain (shown in green) on the ability to see active elastase. When the propeptide was deleted (*lasB6* allele), elastase activity was lost. Complementing the propeptide back (*lasB7* allele) on a plasmid, recovered the elastase activity.

the membrane fraction(McIver, Olson, & Ohman, 1993). These mature domain residues appear to be critical for autocatalysis of the propeptide from the mature domain.

These experiments provided initial insight into the propeptide domain acting as an intramolecular chaperone (IMC) (McIver et al., 1995). An IMC is typically a region of a protein that mediates a conformational change to that protein. This includes the ability of that region (the propeptide) to be essential for proper folding and secretion of the propeptide-mature complex. A number of the M4 propeptides have been thought to function as IMCs.
These previous experiments were initially demonstrated that a TNP family member is an IMC-containing protease. Additionally if this propeptide is a chaperone to the enzyme, it would be expected that the two components would have direct interactions. This was confirmed with co-immunoprecipitation experiments (McIver et al., 1995). Elastase/anti-elastase immunoprecipitates contain the propeptide, as determined by Western blots using propeptide-specific antibodies (data not shown). Furthermore, the non-covalent complex remains associated to permit the complex secretion across the outer membrane (McIver et al., 1995).

The next step involved determining the residues within the propeptide that are required for chaperone activity (McIver, Kessler, & Ohman, 2004). Homology alignments were performed, comparing the propeptide domain with propeptides of other TNPs sequenced at the time. Two regions of interest were found. The first motif, ProM, is near the middle of the propeptide and contains hydrophilic residues. The second motif, ProC, is located at the C-terminus and contains more hydrophobic residues. This conservation suggests an evolutionary relationship of the TNP propeptides to retain essential folding functions. To test whether these conserved motifs were important, single residue substitutions at eight conserved amino acids were introduced on the full-length 3-domain polypeptide and effects were examined. Within the

ProM motif, substitution at R74 resulted in an accumulation of propeptide-mature complex within the cell, suggesting a secretion defect. Substitution at N68 reduced the amount of enzyme in the supernatant as a result of reduced stability of the propeptide-mature complex within the cell. Within the ProC motif, mutations at I181 and A183 again decreased the accumulation of the active enzyme in the supernatant. These mutations generated a phenotype consistent with a defect due to protein folding or stability. Further research on these mutants could elucidate the defective role of these residues as either folding or important for secretion.

α – Lytic Protease and Other Examples of Propeptide-Mediated Folding

The biological behavior of all proteins is managed by adopting specific 3D structures, and understanding these protein-folding mechanisms is currently a noteworthy area of research. Specifically, researchers are examining structure-function relationships. Proteins have been shown to unfold and refold *in vitro*, restoring activity (Wolynes, Onuchic, & Thirumalai, 1995). However, a large group of proteins fail to refold correctly without aid. These molecular chaperones can use peptide-chaperone functions to guide proper folding or ATP hydrolysis to refold misfolded proteins (Nirasawa, Nakajima, Zhang, Yoshida, & Hayashi, 1999; Shinde & Inouye, 1993; Shinde & Inouye, 1996; Shinde & Inouye, 2000; Xu, Horwich, & Sigler, 1997). Propeptide domains are produced by both prokaryotic and eukaryotic organisms (Khalil, 1999). The amino-terminal propeptides are usually located between a signal peptide and then the mature domain. After mediating folding of the mature domain, the propeptides are removed and the properly folded mature domain is found to be at an energy minimum, a state which cannot be attained without the chaperone aid. Detailed examinations have been performed on α-lytic protease to examine its propeptide folding mechanism (Baker, Silen, & Agard, 1992; Baker, Sohl, & Agard, 1992; Sauter, Mau, Rader, & Agard, 1998; Silen, McGrath, Smith, & Agard,

1988; Silen & Agard, 1989; Silen, Frank, Fujishige, Bone, & Agard, 1989; Sohl, Shiau, Rader, Wilk, & Agard, 1997; Sohl, Jaswal, & Agard, 1998).

α-lytic protease (Figure 7) and its propeptide have been extensively examined for its folding and activation mechanism. The presence of the propeptide has been found necessary for secretion and activity of the mature domain by lowering the kinetic barrier of the mature to fold (Silen et al., 1989). A common assumption in protein folding is that native protein states are at a global energy minimum. Alpha-lytic protease, an extracellular serine protease from *Lysobacter enzymogenes*, shatters that assumption. Research has shown that, *in vivo* and *in vitro*, its propeptide region (166 amino acids) is required for the correct folding of the mature domain (199 amino acids) either in *cis* or in *trans* (Silen & Agard, 1989). Experiments aimed at examining the *in vitro* refolding chemically-denatured the mature domain in the absence of pro (Baker, Sohl et al., 1992). This resulted in a folded intermediate. The presence of the propeptide domain led to the rapid formation of the native state of the mature domain. Without the propeptide, the progression of the intermediate to the native folded conformation is blocked by a large kinetic barrier. The rate of folding without the propeptide was measured to be $t_{1/2}$ of ~2,000 years, corresponding to a folding barrier of 30 kcal mol^{-1}. The addition of the propeptide accelerates the rate of mature enzyme folding by a factor of 3×10^9. Furthermore, the rate of unfolding of the native state appears to be slow as well ($t_{1/2}$ of ~1 year), suggesting it is not energetically favorable to unfold once folded correctly. The propeptide is making the mature domain stable and is actually a potent inhibitor of the mature enzyme ($K_i \sim 10^{-10}$ M).

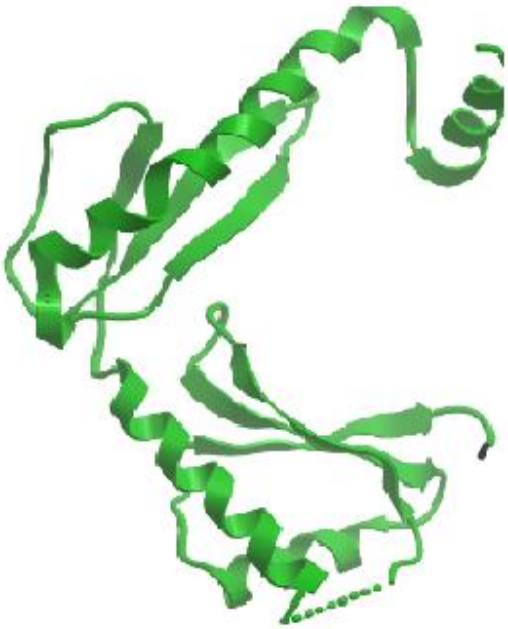

Alpha-lytic protease's propeptide alone

Pro complexed with mature

Figure 7. (A) The ribbon diagram of the propeptide alone of alpha-lytic protease from the bacterium *Lysobacter enzymongenes*.

(B) The ribbon diagram of the propeptide complexed with the mature domain. The two globular regions of the mature domain are shown in purple and blue. The carboxyl terminal residues of the propeptide (green) reside in the active site between the two globular regions.

Deletions made to the propeptide residues, specifically the C-terminal residues, indicate that these residues actively participate in the stabilizing of the intermediate state (Peters et al., 1998; Sohl et al., 1997). The crystal structure of the complex revealed that the propeptide is "C"-shaped and completely surrounds the carboxyl domain of the mature enzyme, protecting the mature domain and allowing it to fold correctly. The propeptide's C-terminal residues actually sit in the active site. The final steps of mature folding take place within the active site. Once complete, the active site cleaves the flexible loop containing the propeptide C-terminal residues; thus the loop is acting as an Achilles heel. This allows for the propeptide to dismantle its foldase role safely from the mature. This important step is followed by rapid proteolytic destruction of the rest of the propeptide, thus releasing the active enzyme.

Scope of this Project

This thesis describes how I further characterized the propeptide of elastase as a "foldase". The proteolytic activity and secretion of elastase is dependent on the ability of the propeptide to act as a chaperone, to aid in the folding of the mature domain, and to works as an inhibitor in order to prevent the activity of the enzyme before secretion. Understanding folding mechanisms can be difficult due to the short-lived intermediate states. However, the two individual components can be manipulated independently and synergistically.

Initial experiments suggest that the propeptide domain alone has a native folded structure. This was accomplished through a number of biochemical and theoretical approaches. The propeptide was examined with circular dichroism and crystallization screens to identify the presence and nature of its secondary structure. Molecular homology modeling provided a visual of what that structure looked like. This model was then used to dock to the crystal structure of the mature domain in order to gain a visual of what the complex could look like. Further

experiments were utilized to characterize the protein-protein interactions between the elastase and propeptide complex. Alignments to other M4 metallopeptidases found a number of conserved residues in the propeptide domain. Numerous alanine substitutions were made and tested for *in vitro* and *in vivo* effects on the ability of the mutated propeptide to aid in folding and secretion of the complex. By testing for *both in vivo* and *in vitro* effects, the mutations could suggest the roles of individual residues as specific for folding *or* secretion. Furthermore, the residues could be localized on the model to see if these critical residues could be reasonable folding mutants or secretion mutants. The identification of the critical residues in the propeptide could lead to a better understanding of how the propeptide acts as a foldase for the mature, working to aid in correct folding and secretion of the complex.

METHODS

Strains used, culture media and conditions. *P. aeruginosa* PAO1 is a clinical isolate from a burn wound used in the Ohman laboratory. *P. aeruginosa* PDO426 [Δ*propeptide*] contains a chromosomal deletion of the propeptide domain only of *lasB* in the lab standard strain PAO1. This was used as an elastase-deficient strain background for expression of the propeptide alleles with mutations. *Escherichia coli* DH5α *fhuA2*Δ*(argF-lacZ)U169 phoA glnV44* Φ*80* Δ*(lacZ)M15 gyrA96 recA1 relA1 endA1 thi-1 hsdR17* (New England Biolabs) was used to propagate DNA which was subjected to site-directed mutagenesis and used in the manipulation of recombinant plasmids. Bacteria were cultured in L broth (1% tryptone, 0.5 % yeast extract, 0.5 % NaCl, pH 7·5) in shaking cultures at 37°C. Unless specified otherwise, antibiotics were used at the following concentrations: ampicillin, 100 μg ml^{-1} for *E. coli*; carbenicillin, 100 μg ml^{-1} for *P. aeruginosa*.

General PCR and recombinant DNA methods. Most routine DNA manipulations were performed as described by Maniatis *et al*. (T. Maniatis, E. F. Fritsch, J. Sambrook, 1982). DNA sequences were determined by the automated technique with custom oligonucleotides (ACGT, Inc). Sequence comparisons were performed using the basic local alignment search tool (BLAST) algorithm, aligned with ClustalW programs and visualized with GoCore software. Enzymes belonging to the TNP family had significant homologies within the protease domain of their molecules.

Recombinant Propeptide Purification. The propeptide domain (lacking pre and mature domains) were over expressed in plasmids pET28b at the NcoI and HindIII sites and encoding an

amino terminal His-6 tag, in *E. coli* BL21 (DE3). Strains were grown to mid-log phase (A_{580}, 0.5 to 0.8). Isopropyl-β-D-thiogalactopyranoside (IPTG) was added to a final concentration of 1 mM and cultures were incubated for an additional 4 h at 37°C with shaking. 250 ml of pelleted cells were resuspended in 10.0 ml fractionation buffer with 8M urea (10 mM Tris-HCl [pH 8.0], 100 mM NaCl). The suspension was stored at –70°C overnight, thawed, and lysed with a French press (twice at 14,000 lb/in^2; Thermo Electron). Cells were centrifuged at 4°C twice at 14,000 x *g* for 20 min. The supernatant was filtered through a 0.45-µm acrodisc filter, and 10.0 ml were applied to an equilibrated nickel resin column (Qiagen). The liquid was allowed to drain by gravity flow. The column was washed four times with 10 ml of wash buffer (fractionation buffer with 50 mM imidazole). His6-Propeptide was eluted stepwise with 500 µl of 1.0 M imidazole in fractionation buffer. Elutes were pooled and dialyzed overnight at 4°C against 10 mM Tris-HCl [pH 8.0], 100 mM NaCl buffer to remove imidazole.

Production of Propeptide Antibody. Polyclonal antisera against recombinant His_6-Propeptide (over expressed as above and sent in a SDS-PAGE piece sample) was generated in New Zealand White rabbits (Immunodynamics, Inc.) and used in a Western immunoblot analysis at a dilution of 1:10,000. Signal detection with chemiluminescent reagents was performed according to the instructions of the manufacturer (Pierce).

Polyacrylamide gel electrophoresis and immunoblot analysis. Protein samples were separated and analyzed on a 12% SDS-polyacrylamide gel electrophoresis (PAGE) (Laemmli, 1970). Protein samples were prepared for SDS-PAGE by heating for 5 min at 100°C in an equal volume of 2X sample buffer (0.1 M Tris-HCl, 5 % SDS, 0.9 % 2-mercaptoethanol (2ME), 20 % glycerol, pH 6.8). Gels were stained with 0.2 % (w/v) Coomassie brilliant blue R-250 (Sigma, St. Louis,

MO) in ethanol: acetic acid: water (30:10:60, v/v/v). A broad-range protein weight marker (Bio-Rad, Hercules, CA) was used for protein size determination. For western blot analysis, proteins were similarly separated by SDS-PAGE and electrophoretically transferred to a nitrocellulose membrane by electroblotting using a Bio-Rad Immuno-Blot assay kit. Antiserum against the purified propeptide was raised in rabbits as described previously. Antiserum against purified elastase was obtained previously in the lab. Detection of the primary antibody on nitrocellulose membranes was revealed with horseradish-peroxidase conjugated goat anti-mouse IgG (Bio-Rad) at a 1:40,000 dilution. Thermo Scientific SuperSignal chemiluminescence reagents were used according to manufacturer's instructions

Purification of active elastase. A *lasB* over expression vector was created by double digestion with NcoI and HindIII of the PCR product wild-type *lasB* gene and placed into a broad host range expression vector pMF54 containing the *trc* promoter and $lacI^Q$ for IPTG induction. When this plasmid (pALH79) was expressed in the Δ*lasB* strain, PDO240, and induced, ten times more elastase was secreted as compared to wild-type. Three liters of this strain was then grown in L broth with maximum aeration at 37°C for 18 hours. Cells were collected by centrifugation and resuspended in fresh media containing IPTG for four hours of protein induction. Cells were removed by centrifugation and the supernatant is filtered to remove cellular debris. Elastase was then precipitated by 60% ammonium sulfate saturation and the pellet was collected by centrifugation. The pellet was resuspended in small volume of 10mM Tris buffer, pH 7.5, dialyzed and applied to an equilibrated DEAE-sepharose column. The column was washed with buffer and then elastase was eluted off with an increase in salt concentration. The fractions

containing the elastase were collected and analyzed for protein concentration via the Bradford assay, activity, and purity.

Elastase Activity Substrates. Proteolytic activity from *Pseudomonas* can be assayed with casein or azocasein whereas elastinolytic activity is determined with elastin–Congo Red or orcein–elastin (Rust, Messing, & Iglewski, 1994). Elastin nutrient agar plate assays can also be used to detect elastase production by *P. aeruginosa* (Rust et al., 1994). However, specific and sensitive elastase activity was determined spectrophotometrically with the fluorogenic substrate Abz-Ala-Gly-Leu-Ala-Nba (Abz: *o*-aminobenzoyl; Nba: 4-nitrobenzylamide) (Bachem).

Assay of *in vivo* enzymatic activity. To obtain standardized cultures of *P. aeruginosa* strains, L broth was inoculated (1:100) with an overnight culture and then grown once the cultures reached an OD_{600} of 0.5. This was then used to inoculate (1:100) 10 ml of L broth and incubated at 37 °C with aeration for 18 h into early stationary phase, at which time extracellular elastase is stable and has reached a plateau. Elastolytic activity in 18 h culture supernatants was determined using a fluorogenic substrate, Abz-Ala-Gly-Leu-Ala-p-Nitro-Benzyl-Amide (Pepnet), which contained a short span of amino acids susceptible to cleavage by elastase surrounded by donor and quencher fluorophores. When this substrate was in the presence of enzyme, the quencher fluorophore was removed and the donor emission is determined. Various concentrations of substrate (final assay concentration = 0.0125 mM - 0.2mM) were prepared in DMSO and added to 0.05M TrisHCl, pH 7.5, 2.5mM $CaCl_2$ buffer in black Costar 96 well plates and prepared in the BioTek FLx800 fluorescence microplate reader. Aliquots of supernatants were added and fluorescence was determined immediately, every 11 seconds for 20 minutes. The excitation and emission wavelengths were 320 and 415 nm respectively. The device was standardized using 2.5 μM quinine sulfate solution. The reaction rates (Relative Fluorescence Units/time) for each

substrate concentration was determined and Lineweaver-Burk plots were constructed to determine K_m values for each propeptide mutant. These values were expressed in molarity (μM). Biological samples were obtained from four different experiments and averaged.

SECTION THREE

The propeptide domain alone folds into a defined structure.

Introduction to Vibriolysin

The M4 family of proteases has been classified in the MEROPS database. Within this family, several of these proteases are initially synthesized as zymogens. These zymogen forms contain propeptides that are essential for proper folding of the mature enzymes. These propeptides are defined as intramolecular chaperones (McIver et al., 1995; Nickerson, Joag, & McGavin, 2008). Members of this family are generally synthesized as pre-proenzymes with an amino-terminal (pre) signal sequence. This domain is then followed by a propeptide domain and finally a mature enzyme domain on the carboxy-terminus.

In addition to elastase, another family member has recently been crystallized that shares homology (51% identity, 68% similarity) to the zymogen form of elastase (Gao et al., 2010). This new zymogen is vibriolysin, a thermolysin-like protease. Vibriolysin MCP-02 was isolated from *Pseudoalteromonas* species SM9913: the mature domain and inactive complex were crystallized and archived in the Protein Database (mature: 3NQX, inactive complex: 3NQY). The zymogen structure of vibriolysin is similar to the zymogen of pro-elastase. Both have a 23 amino acid signal peptide at the amino-terminus. Both have a long propeptide (vibriolysin's is 180 amino acids while elastase's is 174) that contains the two fold regions of conservation: the FTP (fungalysin/thermolysin propeptide) domain and the PepSY (peptidase propeptide inhibitor) domain. Vibriolysin's mature domain is 315 amino acids in length, and it is composed of two globular domains linked together. Between the two globular domains is the conserved HEXXH motif that coordinates zinc atom. The catalytic residue Glu346 is the second residue in the

HEXXH motif, similar in elastase. Vibriolysin, however, contains an additional carboxyl-terminal domain, PPC (bacterial pre-peptidase C-terminal domain). These crystallization and biochemical studies however were performed with variations of the enzymes that lacked this PPC domain. The domain has been found at the carboxyl-terminus of certain secreted bacterial peptidases, but these are not present in the active peptidase form.

The similarity between the two zymogens suggested the propeptide from elastase would function by an analogous mechanism. The two propeptide domains (Figure 8) aligned with a high degree of identity (32%) and similarity (52%), particularly in the two conserved fold regions, FTP and PepSY. When the whole zymogens were aligned (Figure 9), the sequence identity was 51% and the sequence similarity was 68%. This provided a strong rationale for performing a number of biochemical experiments to determine if the propeptide from elastase had native structure. The first approach utilized was circular dichroism.

Circular dichroism results

Circular dichroism (CD) is the differential absorption of left- and right-handed circularly polarized light. When polarized light (at selected wavelengths) reaches the molecule, the two types are absorbed to different extents, and this difference is measured yielding the CD spectrum of the sample (Dodero, Quirolo, & Sequeira, 2011). Three recombinant amino terminal histidine tagged propeptide samples were purified and dialyzed overnight in 5 mM phosphate buffer, and the CD spectrum average (Figure 10) was then obtained using a Jasco J-720 spectrometer equipped with a thermal peltier temperature control module (University of Richmond, Dr. Dattelbaum). All the measurements were performed using protein solutions of 1 uM in 5 mM phosphate buffer (pH 7.0 at 25°C) and analyzed by the spectrometer's Spectra Manager software

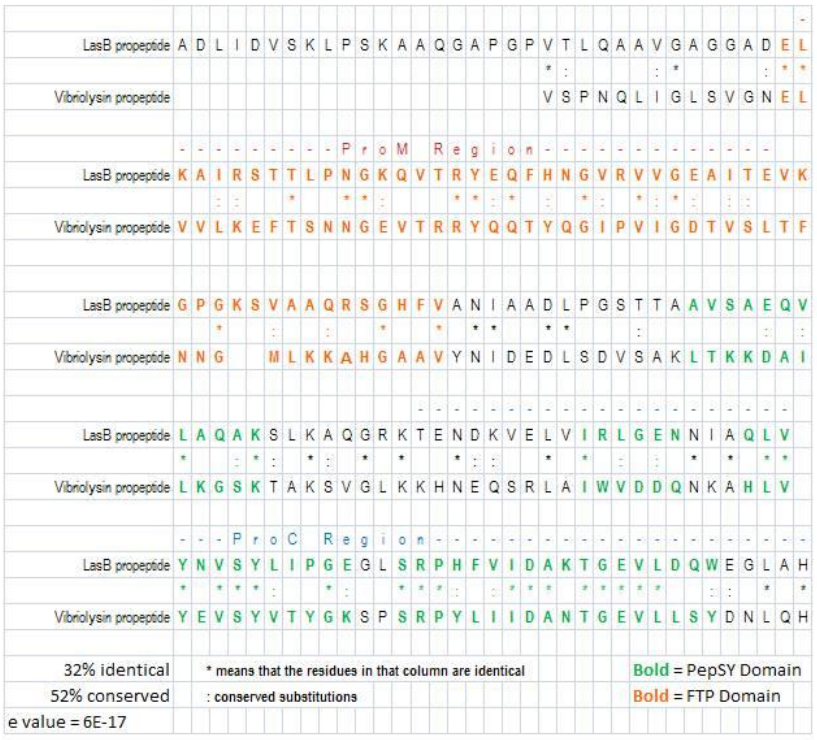
LasB propeptide
Vibriolysin propeptide
ProM Region
LasB propeptide
Vibriolysin propeptide
LasB propeptide
Vibriolysin propeptide
ProC Region
LasB propeptide
Vibriolysin propeptide
32% identical
52% conserved
e value = 6E-17
* means that the residues in that column are identical
: conserved substitutions
Bold = PepSY Domain
Bold = FTP Domain

Figure 8. This is the sequence alignment of the propeptide domain of elastase (LasB) and the propeptide domain of vibriolysin. The residues in orange are those in the Fungalysin-Thermolysin propeptide domain, and those in green are in the PepSY domain. The ProM region is highlighted above the residues indicated in red. The ProC region is highlighted in blue. Residues that were identical were labeled with an "*". Those residues that were conserved in the alignment were labeled with an ":".

(Propeptides aligned same as previous figure)																																			
Mature domains																																			
Elastase	A	E	A	G	G	P	G	G	N	Q	K	I	G	K	Y	T	Y	G	S	D	Y	G	P	L	I	V	N	D	R	C	E	M	D	D	G
	*		*		*	*	*	*	*		*		*	*	*		*	*	:	*	:			*		*	:	:		*		*	:	:	
Vibriolysin	A	N	A	T	G	P	G	G	N	L	K	T	G	K	Y	L	Y	G	T	D	F	D	S	L	D	V	S	N	T	C	S	M	N	N	A
Elastase	N	V	I	T	V	D	M	N	S	S	T	D	D	S	K	T	T	P	F	R	F	A	C	P	T	N	T	Y	K	Q	V	N	G	A	Y
	*	*		*	:	:	:	*			*			*		:	:		:		*		*	*		*	*	:	*	:	:	*	*	*	*
Vibriolysin	N	V	R	T	I	N	L	N	G	G	T	-	-	S	G	S	S	A	Y	S	F	T	C	P	E	N	T	F	K	E	I	N	G	A	Y
Elastase	S	P	L	N	D	A	H	F	F	G	G	V	V	F	K	L	Y	R	D	W	F	G	T	S	P	L	T	H	K	L	Y	M	K	V	H
	*	*	*	*	*	*	*	*	*	*		*	:	*		:	*		*	*		*	*	:	*	*	:		:	*		*	:	*	*
Vibriolysin	S	P	L	N	D	A	H	F	F	G	N	V	I	F	N	M	Y	N	D	W	L	G	T	A	P	L	S	F	Q	L	Q	M	R	V	H
Elastase	Y	G	R	S	V	E	N	A	Y	W	D	G	T	A	M	L	F	G	D	G	A	T	M	F	Y	P	L	V	S	L	D	V	A	A	H
	*			:		*	*	*	:	*	*	*	:	*	*		*	*	*	*				*	*	*	*	*	*	*	*	*	:	*	*
Vibriolysin	Y	S	S	N	Y	E	N	A	F	W	D	G	S	A	M	T	F	G	D	G	Q	N	T	F	Y	P	L	V	S	L	D	V	S	A	H
Elastase	E	V	S	H	G	F	T	E	Q	N	S	G	L	I	Y	R	G	Q	S	G	G	M	N	E	A	F	S	D	M	A	G	E	A	A	E
	*	*	*	*	*	*	*	*	*	*	*	*	*	*	*		*	:		*	*	:	*	*	*	*	*	*	*	*	*	*	*	*	*
Vibriolysin	E	V	S	H	G	F	T	E	Q	N	S	G	L	I	Y	N	G	K	P	G	G	L	N	E	A	F	S	D	M	A	G	E	A	A	E
Elastase	F	Y	M	R	G	K	N	D	F	L	I	G	Y	D	I	K	K	G	S	G	A	L	R	Y	M	D	Q	P	S	R	D	G	R	S	I
	*	*	*	:	*		*	*	:	*	:	*		*	*		*	*	:	*	*	*	*	*	*	:		*	:	:	*	*	*	*	*
Vibriolysin	F	Y	M	K	G	S	N	D	W	L	V	G	K	D	I	F	K	G	N	G	A	L	R	Y	M	N	N	P	T	Q	D	G	R	S	I
Elastase	D	N	A	S	Q	Y	Y	N	G	I	D	V	H	H	S	S	G	V	Y	N	R	A	F	Y	L	L	A	N	S	P	G	W	D	T	R
	*	*		*		*	*	:	*	:	*	*	*	:	*	*	*	*	*	*		*	*	*		*	*		:	*	*	*	*	*	:
Vibriolysin	D	N	Q	S	N	Y	Y	S	G	M	D	V	H	Y	S	S	G	V	Y	N	K	A	F	Y	N	L	A	T	T	P	G	W	D	T	Q
Elastase	K	A	F	E	V	F	V	D	A	N	R	Y	Y	W	T	A	T	S	N	Y	N	S	G	A	C	G	V	I	R	S	A	Q	N	R	N
	*	*	*		*				*	*	:		*	*	:	*				:	:					*	*	:		:	*		:		*
Vibriolysin	K	A	F	I	V	M	A	R	A	N	Q	L	Y	W	S	A	G	V	G	W	D	L	A	G	N	G	V	M	D	A	A	C	D	L	N
Elastase	Y	S	A	A	D	V	T	R	A	F	S	T	V	G	V																				
	*				*	*			*		:		*	*	*																				
Vibriolysin	Y	D	P	N	D	V	K	A	A	L	A	A	V	G	V																				
51% identical	* means that the residues in that column are identical																																		
68% conserved	: conserved substitutions																																		
E value = 9e-133																																			

Figure 9. Shown is the alignment of the mature domains of elastase and vibriolysin. The propeptide region is shown in Figure 8 and remains the same when the whole gene product is aligned. Residues that were identical were labeled with an "*" and conserved in the alignment were labeled with an ":".

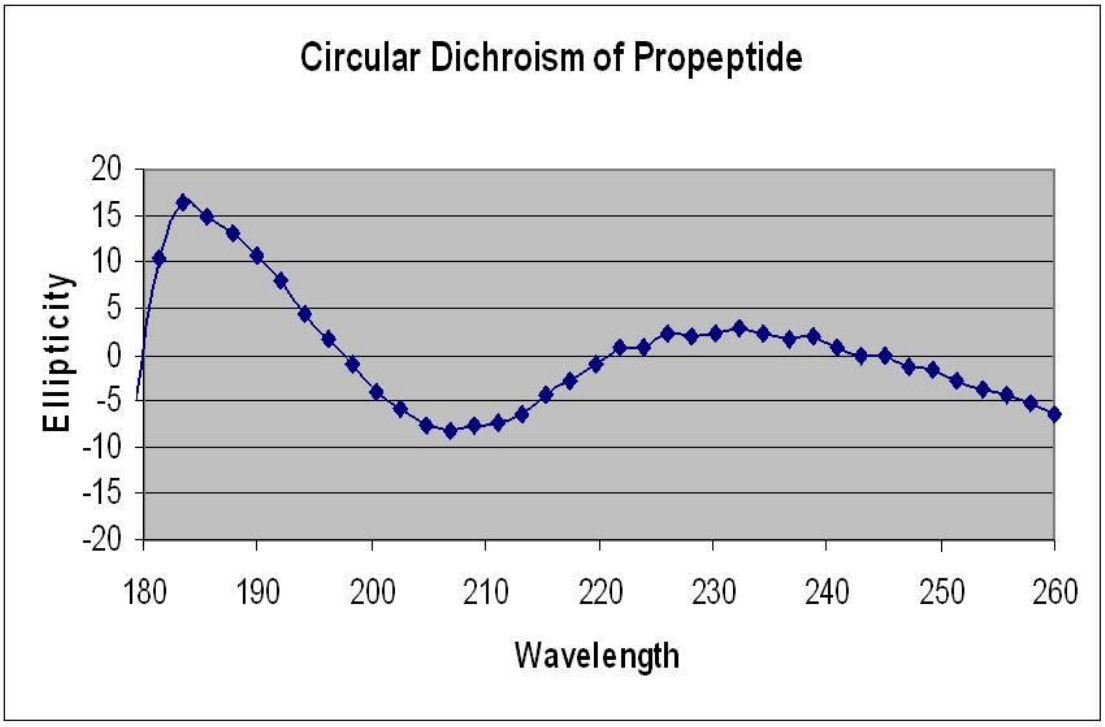
Circular Dichroism of Propeptide
Ellipticity
20
15
10
5
0
-5
-10
-15
-20
180
190
200
210
220
230
240
250
260
Wavelength

Figure 10. The circular dichroism analysis of the purified recombinant propeptide, which suggests has a predominantly beta strand conformation. The graph shows the wavelengths across the x axis at which the ellipticity (y axis) was obtained. This is an average of three measurements on propeptide samples performed in 5 mM phosphate buffer (pH 7.0) at room temperature.

(ver. 5.1.0.0). This confirmed it was composed primarily of beta strands. The circular dichroism signature is 51% beta strands; the remaining is alpha helices and random coils. Further analysis (K2d web server algorithms) of the propeptide's raw data suggests this CD signature is composed of primarily beta strands. The circular dichroism data obtained gave confidence to proceed to the next biochemical step which would focus on identifying if the propeptide domain alone could grow crystals as for x-ray crystallization.

Crystallization screen results

Based on the suggested presence of a defined structure for the propeptide domain alone, recombinant propeptide was purified and sent to Hauptman-Woodward Medical Research Institute for inclusion in their **high-throughput screening (HTS) laboratory (Luft et al., 2003).** The lab prepares crystal-growth screening experiments in 1536-well microassay plates for propeptide crystallization screening. Amino terminal histidine tagged propeptide samples (600 microliters) at a concentration of 10 mg/ml were prepared and sent to the institute. Aliquots of the propeptide protein were then mixed individually with 1536 unique crystallization cocktails (provided by Hampton Research) by a robotic system for the microbatch-under-oil crystallization method. Each cocktail condition, each in its own well, was then imaged several times (at day 1, week 1, week 2, week 3, week 4, week 5, and week 6). These images could then be viewed and determined if crystals have grown.

Several conditions produced crystals, and these crystals grew larger as the weeks passed. The largest of the crystals (Figure 11A) was seen at week 4. The cocktail reagent for this well was 1.6 M Ammonium Sulfate, 0.1 M MES monohydrate, 10% 1,4-Dioxane. Additional wells produced large crystals, and some of these can be seen in Figure 11B-E. The ability of the propeptide to generate crystals under a variety of conditions suggests the propeptide has a

A

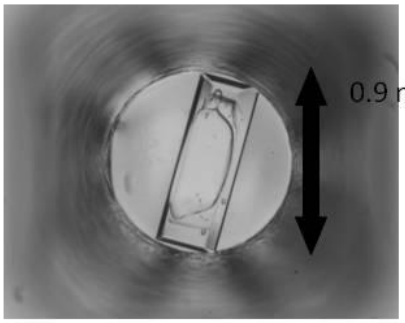

B C D E

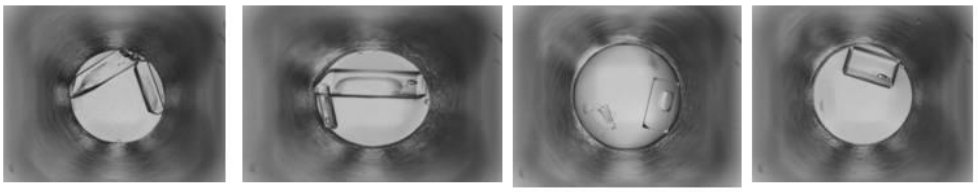

Figure 11. Images of elastase were obtained of the different crystallization cocktails at week 4. These are shown as A-E. The dimension of the well are as labeled. The diameter of each well is 0.9 mm. Cocktail condition for well A is 1.6 M Ammonium Sulfate, 0.1 M MES monohydrate, 10% 1,4-Dioxane. The cocktail condition for well B is HR Grid Screen Salt HT-A10 -- 1.6 M Ammonium sulfate, 0.1 M HEPES, pH 7.0. The cocktail condition for well C is HR Grid Screen Salt HT-B2 – 2.4 M Ammonium sulfate, 0.1 M Citric acid, pH 5.0. The cocktail condition for well D is HR Grid Screen Salt HT-H12 – 4 M Sodium chloride, 0.1 M BICINE, pH 9.0. Finally, the cocktail condition for well E is HR HT Screen G8 – 0.1 M Sodium Chloride, 0.1 M HEPES, 1.6 M Ammonium Sulfate, pH 7.5.

defined structure. To examine what the structure could look like, molecular modeling methods were next employed.

Molecular modeling results

Having already determined that the propeptide sequence of elastase aligns with the sequence of the propeptide of vibriolysin from *Pseudoalteromonas* sp. SM9913, this allowed me to use molecular modeling techniques to obtain a structure for the propeptide of elastase. This was accomplished using FUGUE. FUGUE assesses sequence similarity, but then quantifies these similarities in the context of a known 3D structure; it defines a structural environment in terms of main-chain conformation, secondary structure, solvent accessibility and also hydrogen bonding status. FUGUE uses environmentally specific substitution tables and structure-dependent gap penalties, where scores for amino acid matching and insertions/deletions are evaluated depending on the local environment of each amino acid residue in a known structure (Shi, Blundell, & Mizuguchi, 2001). Utilizing the ORCHESTRAR homology modeling program in the SYBYL software package, a 3D model of the propeptide was built by first modeling conserved cores, then variable regions (loops), based on the FUGUE predicted homolog. Side chains were added and finally the energy was minimized in SYBYL, which is able to remove steric clashes at the subunit interfaces (Dolan, Keil, & Baker, 2008).

The FUGUE database scans all the structures in the Protein Database and provided a structural homolog with a high homology score (28.5). A FUGUE Z-score of 6 gives a 99% confidence analysis the unknown structure will align to the known structure (Shi et al., 2001). The propeptide sequence was 32% identity with its identified homolog, vibriolysin from *Pseudoalteromonas* sp. SM9913. FUGUE analyzed the two propeptides that contained both the

A

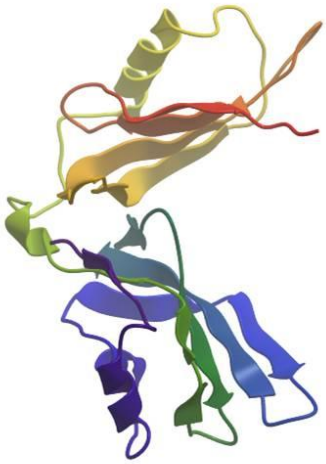

B

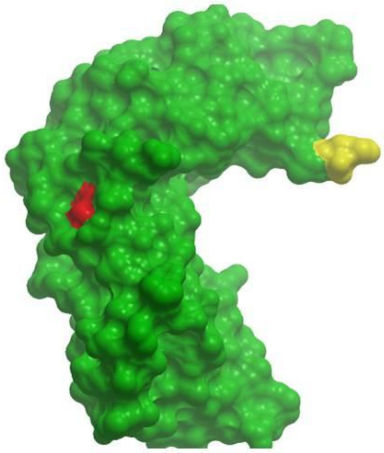

Figure 12. A model of elastase based on the structure of the vibriolysin propeptide was created of the propeptide domain alone. (A) Shown is a ribbon diagram with the beta strands and alpha helices highlighted. (B) Shown is a space filled representation, with amino-terminal alanine residue highlighted in red and the carboxy-terminal histidine residue highlighted in yellow.

FTP and PepSY folds. Modeling programs then built the structure of the propeptide around the known crystal structure of vibriolysin's propeptide and assessed the fit. The propeptide of elastase has a high confidence analysis when analyzed by I-TASSER program (Zhang, 2008) as well. This I- TASSER server performs the same search as FUGUE and generates a model (Figure 12). It then matches the predicted 3D model to the known structures in 3 independent libraries (consisting of proteins of known enzyme classification number, gene ontology vocabulary, and finally ligand-binding sites) and generates a TM-score in a range of -5 to +2. The TM-score for the model of the elastase propeptide was +0.93. The model also confirmed the presence of primarily beta strands (Figure 12A indicated with large wide arrows).

Molecular model Docking results

Once a model of the propeptide's 3D structure was generated and analyzed, it could then be used to predict the propeptide-mature complex structure. The Hex protein docking server constrains a structure in a 3D field and uses charge and size of the residues on the structures to fit the other structure into a predicted 3D complex (Ritchie, 2008). In this case, the crystal structure of mature elastase was constrained, and the propeptide model was assessed at various positions around the mature domain. One such resulting complex (Figure 13A) was very similar to the complex (Figure 13B) of the propeptide and mature domains of Vibriolysin. In both these structures, the propeptide's carboxy-terminal residue is a histidine and it resides in the active site of the mature domains. In addition, the propeptides appear to be a "C" shape, which cups around carboxyl globular domain of the mature.

To confirm that the propeptide of elastase can function as an intramolecular chaperone, it was critical to first establish that it has a native structure providing stability to the complex. A number of biochemical and theoretical approaches were utilized to determine the presence of a

A

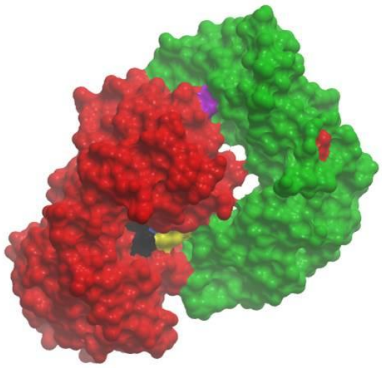

B

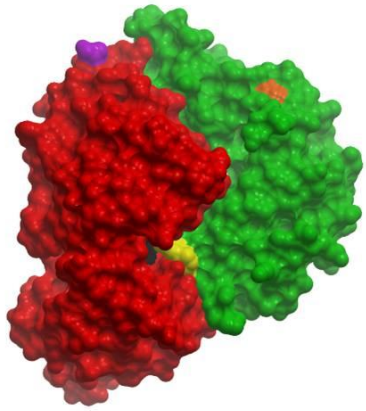

Figure 13. The elastase propeptide model was docked to the 3D structure of the mature active enzyme using the Hex protein docking server. Space filling representations were used for both the (A) propeptide-elastase complex and the (B) propeptide-vibriolysin complex. The propeptide domains are shown in green with its amino-terminal residue show in dark orange and its carboxy-terminal residue in yellow. The mature domains are shown in red with the active site residues in black and the carboxy-terminal residue in purple.

native secondary structure and its type. The evidence from the circular dichroism experiments and molecular modeling suggest the propeptide primarily has a beta sheet conformation. The docking model enables a visual interpretation of how the propeptide could be interacting with the mature domain and these will be helpful in the next series of experiments in which the roles of individual conserved residues in the propeptide domain are determined.

SECTION 4

The propeptide has conserved residues that affect folding and activation of the mature

Alignment of the propeptide to other M4 metalloprotease propeptides

The previous research on the role of elastase's propeptide established that it was required for folding and secretion of the mature domain. From my previous experiments that suggest the propeptide had a defined structure, one could deduce that there are critical residues in this structure important for the folding and activation of the mature domain. To narrow down the residues which could be critical, a sequence alignment of the propeptide from elastase to other propeptides of M4 metalloproteases was performed in order to identify those conserved among the different propeptides.

Propeptides with homology to the elastase propeptide were first identified by a search of the protein database using Basic Local Alignment Search Tool (BLAST). The amino acid sequences for the propeptide were then aligned (Figure 14) to the elastase propeptide according to the BLAST results using the NCBI ClustalW server(Thompson, Higgins, & Gibson, 1994). The sequences found by the BLAST are: elastase LasB of *P. aeruginosa* (LasB); Class 4 metalloprotease of *Chromobacterium violaceum* (Class 4 metalloprotease); metalloprotease from *Listonella anguillarum* (metalloproteinase); neutral protease/zince metalloprotease from *Salinivibrio proteolyticus* (neutral protease); VtpA protease from *Vibrio tubiashii (*VTPA); hemagglutinin/proteinase of *V. cholerae* (hemagglutinin/proteinase); protease from *Aeromonas punctata* (protease); proaminopeptidase protease from *Aeromonas punctata* (pro-aminopeptidase); and M4 peptidase or thermolysin like enzyme from *Shewanella baltica* (M4 peptidase/thermolysin).

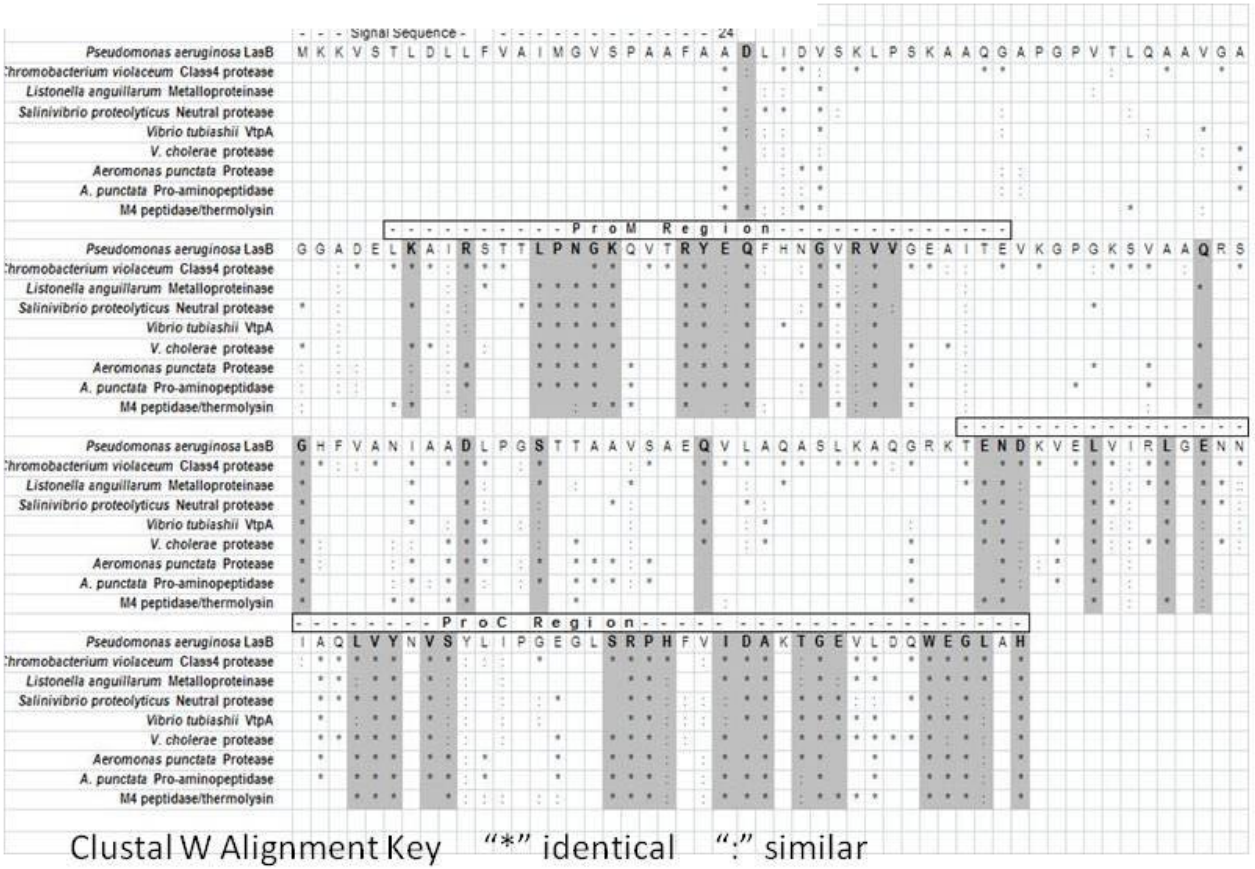
Signal Sequence
24
ProM Region
ProC Region
Pseudomonas aeruginosa LasB
Chromobacterium violaceum Class4 protease
Listonella anguillarum Metalloproteinase
Salinivibrio proteolyticus Neutral protease
Vibrio tubiashii VtpA
V. cholerae protease
Aeromonas punctata Protease
A. punctata Pro-aminopeptidase
M4 peptidase/thermolysin
Clustal W Alignment Key "*" identical ":" similar

Figure 14. A BLAST search with the elastase propeptide sequence and ClustalW alignment indicates there are conserved residues among the propeptides. A "*" symbol indicates amino acid identity; a ":" symbol indicates similarity; empty spaces represent gaps in similarity introduced by the ClustalW alignment program. Residues in bold are those chosen based on conservation and selected for mutation. The regions were designated ProM and ProC, and the signal sequence is depicted with the first residue of the propeptide numbered 24. The sequences shown are the propeptides of : elastase LasB of *P. aeruginosa* (LasB); Class 4 metalloprotease of *Chromobacterium violaceum* (Class 4 metalloprotease); metalloprotease from *Listonella anguillarum* (metalloproteinase); neutral protease/zince metalloprotease from *Salinivibrio proteolyticus* (neutral protease); VtpA protease from *Vibrio tubiashii (*VTPA); hemagglutinin/proteinase of *V. cholerae* (hemagglutinin/proteinase); protease from *Aeromonas punctata* (protease); proaminopeptidase protease from *Aeromonas punctata* (pro-aminopeptidase); and M4 peptidase or thermolysin like enzyme from *Shewanella baltica* (M4 peptidase/thermolysin).

Those residues boxed in grey were then chosen based on conservation and were mutated to alanines. By investigating the phenotype of the conserved residues, the ability of the propeptide to fold and activate the mature domain will be indicated in the final elastase activity.

Construction of mutants in the propeptide alleles to operate in *trans*

The construction of these alleles encoding the alanine substitutions in the propeptide sequence was performed via oligonucleotide-directed site-specific mutagenesis. This PCR technique was based on the QuikChange Site-Directed Mutagenesis system (Stratagene) as described by the manufacturer. Single-base-pair substitutions encoding mutant propeptide residues were introduced within the plasmid pVM8. This template plasmid contained the wild-type *lasB* gene signal sequence domain and regulatory region on a 2·5 kb *Eco*RI–*Pst*I fragment in pUCP19 and lacked the mature domain of the gene and encoded for a stop codon after the propeptide domain. The original wild-type methylated plasmid, pVM8, was used in the PCR steps. DpnI was then used to cleave the template strain and the mutated plasmid was transformed into DH5α cells. Site-specific substitutions were verified by DNA sequence analysis to generate the pEB40 series of plasmids. These pEB40 clones were mobilized into the *P. aeruginosa lasB*-deficient strain PDO426 by triparental mating with HB101 (pRK2013)(Figure 15). Plasmid pVM8, with the wild-type *lasB* propeptide domain in the plasmid pUCP19, was used as a positive control. The empty vector pUCP19 was used as a negative control.

The utilization of the ability of the propeptide to act in *trans* on the mature domain is beneficial to this assay. The single substitutions of conserved residues to alanine on the propeptide were generated and the plasmids were introduced to the background strain. Both the pre-mature and the pre-pro alleles kept the native promoter for the gene. The *Pseudomonas* host

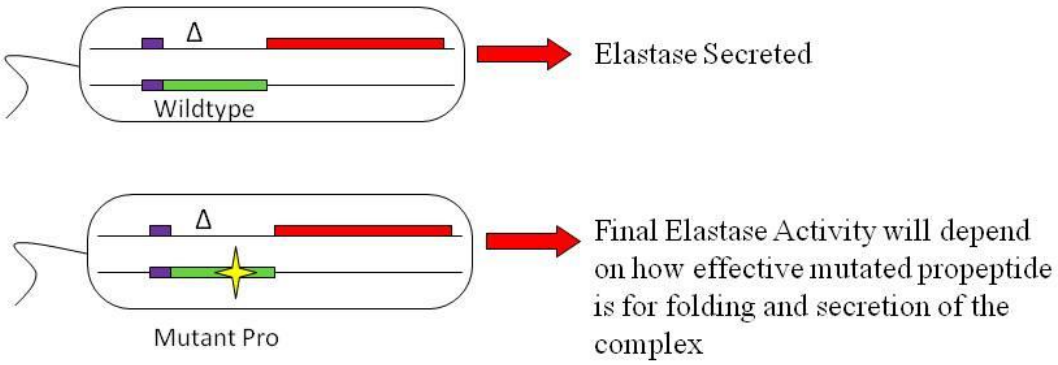

Background strain lacks the propeptide on the chromosome PDO426.

The propeptide alleles are in trans on the pVM8 and pEB40 plasmids

Figure 15. This figure depicts the schematic used to measure the effects of the mutated propeptides on elastase *in vivo*. The background strain lacks the propeptide domain only (PDO426) and the propeptide is brought in *trans* by either pVM8 (wild-type) or the pEB40 plasmids (alanine substituted mutant propeptide alleles).

used the quorum-sensing regulation systems to synthesize the two components. The two components could then translocate through the inner membrane. The mutated residues in the propeptide interact with the mature domain within the periplasmic space. The complex was then secreted and the elastase activity was assessed in the supernatant (protocol described in the Methods). A range of substrate concentrations was utilized to obtain the K_M value for each propeptide. This allowed for the comparison of the wild-type propeptide to the mutant propeptide's ability to fold and secrete the mature domain without the final secreted enzyme concentration as a factor.

Assessment of those mutant propeptides *in vivo*

The ability to measure the kinetics of the enzyme (the enzyme's affinity for the substrate) without the concentration of enzyme as a factor is critical for this analysis. Those mutant residues that have little effect on the folding and secretion of the complex act like wild-type propeptide and yield similar K_M values (substrate affinity values). However, if the mutant propeptide residues have an effect on the ability to fold, activate and secrete the mature domain, the effect could be so drastic that the misfolded complex accumulates in the cell and is eventually degraded with so little to no activity is measured outside the cell.

First order Michaelis-Menten kinetics describes the affinity between the enzyme and the substrate (Kou, Cherayil, Min, English, & Xie, 2005). The K_M value is the inverse of the enzyme affinity for the substrate. The enzyme affinity for the substrate will reflect how the propeptide aids in folding and secretion. By harvesting the enzyme at the peak of its production, the enzyme is assumed to have completed its interaction with the propeptide and thus free to cleave the substrate. Utilizing the sensitive fluorogenic substrate, determination of even minimal quantities of elastase in the medium, and quantifying of K_M values was allowed. The enzyme's

A

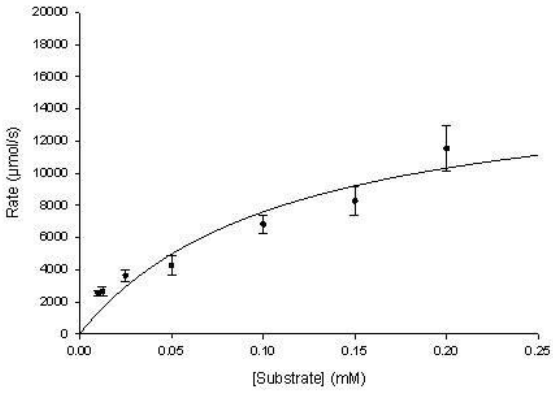

B

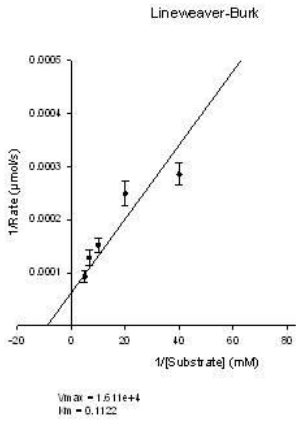

Km = 0.11mM
Optimum [substrate]

Figure 16. Wild-type elastase was used to determine the affinity for the fluorogenic substrate. A range of final substrate concentrations were used to determine the reaction rates and plotted in the (A) Michealis-Menten graph. This graph indicates the enzyme is undergoing first-order single substrate enzyme kinetics. The inverse of the reaction rates and the inverse of the substrate concentrations were plotted in the (B) Lineweaver-Burk plot to yield the Km value (the inverse of where the linear regression passes through the x axis) = 0.11 mM.

concentrations were nefated and comparisions of how the residues in the propeptide affected the enzyme's activation were able to be made.

Initial experiments were performed to determine the optimal substrate concentrations used to assay the mutants. Wild-type elastase was tested with a range of substrate concentrations and the rate of each reaction at the individual substrate concentrations, was plotted in the Michaelis-Menten diagram (Figure 16A). The inverse of reaction rates and the inverse of the substrate concentrations were then plotted in a Lineweaver-Burk plot (Figure 16B) to determine the K_M. A linear regression through the points was generated, and the inverse of the X axis value yielded the K_M. A previously published experiment determined the K_M value for elastase and this specific fluorogenic substrate to be 0.11 mM (Nishino & Powers, 1980). The value obtained was also 0.11 mM. Then a range of substrate concentrations encompassing the K_M were employed to test the different propeptide mutant alleles. In the assay, the enzyme samples were tested with the final substrate concentrations of 0.0125 mM, 0.025 mM, 0.05 mM, 0.1 mM, 0.15 mM, and 0.2 mM to provide the different reaction rates. These rates were then assembled into Lineweaver-Burk plots in order to assess each mutant's effect on mature activity. If the mutatated residue in the propeptide had minimal effect, then the closer the K_M value was to wild-type. The more damaging the effect of the mutated residue, the larger the K_M value grew, indicating a poor average affinity of the enzyme for the substrate.

A bar graph (Figure 17) was constructed to display the K_M values. Because the residues that were chosen were conserved it is not surprising that all of the mutant propeptides had an impact on the K_M value of resulting enzyme, with some more than others. Mutations to the G69, E143, P177, H178, and E187 residues had values closer to wild-type, implying these residues were less important for propeptide-mature interaction.

Fold change of the Mutant Km values to the Wildtype Km value
Propeptide Residue
in vivo Table
0
10
20
30
40
50
60
70
80
D25A
I59A
P62A
L66A
P67A
N68A
G69A
G69D
K70A
R74A
V75A
E76A
Q77A
G81A
R83A
V84A
V85A
Q102A
G105A
D114A
S118A
Q127A
E143A
N144A
D145A
L149A
L153A
E155A
L161A
V162A
V163
V165A
S166A
S175A
P176A
P177A
H178A
I181A
D182A
A183G
T185A
G186A
E187A
W192A
E193A
G194A
L195A
H197A

Figure 17. The fold change of the K_M values are depicted for the *in vivo* analysis. The mutant elastase propeptide alleles K_M values were expressed as fold change from the wild-type K_M value. The blue asterisk indicated residues that were unable to produce enzyme activity to determine the K_M.

Mutations, however, to a large number of other propeptide residues caused a large value change in K_M, indicating that those elastase variants had less affinity for the substrate. These propeptides had a diminished capacity to aid in the folding of the complex. These propeptides include D25, K59, R62, L66, P67, K70, R74, Y75, E76, Q77, G81, R83, V84, V85, G105, D114, S118, Q127, N144, D145, L149, L153, E155, L161, V162, Y163, V165, S166, S175, I181, D182, A183, G186, W192, E193, G194, and L195. Each of these mutant propeptides caused at least a 10-fold difference to the K_M compared to wild-type.

There were five mutants that produced so little active enzyme that the K_M value could not be determined. These were indicated as a blue asterisk on the bar graph "*". These residues included N68A, Q102A, R176A, T185A, and H197A. Each of these residues appears to be polar and could be essential for protein-protein interactions.

These conserved residues that were mutated and shown to affect the affinity of the enzyme to the substrate could be impacting mature elastase in several different ways. There could be residues that are found in the interior of the propeptide and help stabilize the propeptide's structure. Residues could lie on the exterior of the propeptide and be important for recognition for the complex by the Type 2 transport system. Additionally, there could be residues that reside at the interface of the propeptide-mature complex that provide anchors for the mature domain. Disrupting any of these residues could impact the K_M value of the resulting enzyme.

Construction of mutant propeptides to be expressed as recombinant propeptides

In order to separate the role of the individual residues, several residues were chosen from the *in vivo* data. Propeptides with residues that produced fold-changes of at least 50-fold difference, as well as those for which K_M values could not be determined, were chosen for the

next set of experiments. These residues include R62, L66, P67, N68, R74, Q102, S118, Q127, N144, D145, R176, T185, W192, E193, G194, L195, and H197 for the Propeptide – Mediated *In vitro* Foldase Activity Assay.

This assay (Figure 18) utilized recombinant propeptide and active elastase that were denatured individually and then renatured together at 4°C. The renatured enzyme was then assayed as before using the fluorogenic substrate. The active enzyme was purified from the supernatants of *Pseudomonas* cultures and tested for initial activity. Recombinant propeptide (wild-type and mutants) were generated with an amino-terminal histidine tag. However, the template plasmid was pEB2, which encodes a signal sequence, a histidine tag, a thombin cleavage site and the propeptide domain alone in the pET28b vector (see Methods). This allowed for the purification of the mutant recombinant propeptides on a nickel column.

Once the two individual components were purified, they were denatured using 6 M Guanidine-HCl, which allowed for the now inactive enzyme to retain its disulphide bonds. The two denatured components were mixed together at a 1:1 ratio of 3 µM each and dialyzed against 0.05 M TrisHCl (pH 7.0) at 4°C, with the buffer changed four times each hour. An aliquot was taken and combined trypsin to ensure the propeptide degraded and the active site was now clear. The sample was then assayed using the same protocol as the *in vivo* assay, replacing the quantity of supernatant with the same quantity of refolded sample. The enzyme was mixed with buffer, and the range of substrate concentrations and the K_M were evaluated. The K_M value here allows for an assay without knowing the concentration of enzyme.

Guanidine HCl
-S-S-
Active Elastase
Denatured Elastase
Mix 1:1
and
Dialyze
Active Elastase
Guanidine HCl
Propeptide
Denatured Pro
Inactive
Elastase-Pro
Complex

Figure 18. Shown is a schematic of the propeptide-mediated *in vitro* foldase activity assay for elastase. Active elastase enzyme is denatured with guanidine HCl. Recombinant propeptide is denatured as well. These two components are then mixed 1:1 and dialyzed against TrisHCl buffer to dialyze away the guanidine HCl, allowing the two proteins to complex and fold. The final activity of the enzyme can then be assayed as a reflection of how well the mutant propeptide aided in folding alone.

Assessment of the mutant recombinant propeptides *in vitro*

By utilizing this *in vitro* assay, the effects of the propeptide on secretion can be ignored. This is similar to examining what is happening in the periplasm before the complex is recognized by the secretion system. These mutant propeptides are only now able to fold into the propeptide's secondary structure and complex with mature domain. These allowed for the classification of several residues in the propeptide that could be important for secretion recognition, i.e., these propeptides produced near wild-type K_M values now they are free from the secretion apparatus even though in the *in vivo* assay they had drastic effects.

The K_M values are depicted in a bar graph (Figure 19). Alanine substitutions at N68, S118, Q127, D145 and T185 had values similar to the wild-type propeptide. This suggests that these substitutions only function similarly to wild-type since they aren't required to be recognized by the secretion apparatus. However, residues such as R62 L66, P67, R74, N144, W192, E193, G194, and L195 again had large differences between their K_M values and that of wild-type. These residues could be critical for the propeptide's stability or exist at the interface when complexed with mature and are now unable to perform their function.
Several residues (Q102, R176, and H197) were unable to fold elastase in vitro into native structure and their K_M values could not be determined. This suggests these residues are essential for their role in folding the mature domain into active enzyme.

These conserved residues, discovered by alignment to other M4 metalloproteases, appear to be vital for the maturation and activation of the enzyme. Diminished enzyme activity was found in both the *in vivo* and the *in vitro* assays. Three dimensional examination of the location of these residues within the complex would allow for the surrounding environment of the residues to be further explored.

in vitro Table
Fold change to Wildtype Extracellular Elastolytic Activity
70
60
50
40
30
20
10
0
R62A
L66A
P67A
N68A
R74A
Q102A
S118A
Q127A
N144A
D145A
R176A
T185A
W192A
E193A
G194A
L195A
H197A
Propeptide Residue

Figure 19. The fold changes of the K_M values for elastase variants are depicted. The mutant recombinant propeptide K_M values were expressed as fold change from the wild-type K_M value. The red asterisk indicated residues that were unable to produce enzyme activity to determine the K_M.

SECTION 5

The mutant residues in the propeptide are in critical 3D locations to function.

Determining the role of individual residues within the propeptide

Substitutions in several of the conserved residues were found to have a deleterious effect on the ability of the mature enzyme to fold, activate or be recognized by the secretion apparatus. An analysis of the ability of the propeptide within the cell to recover the mature domain's activity in *trans* provided further confirmation that the propeptide was acting as an intramolecular chaperone. Additionally, these mutant residues were examined outside the cell to provide insight into the individual roles the residues could be playing.

To further clarify the potential roles of the individual residues, a bar graph of both sets of data (Figure 20) was developed. The data provided by *in vivo* analysis (Figure 17) is shown in blue bars with blue asterisks indicating values not determinable due to the absence of enzyme. The data provided in the *in vitro* analysis (Figure 19) is shown in red bars and red asterisks. Here one can now compare how an individual residue performed in each case. For instance, R62 when mutated to alanine, performed poorly in both the cell system and the cell-free system. Additional members of this group include L66, P67, R74, N144, W192, E193, G194, and L195. These propeptides with substitutions did not perform better when the enzyme and mutant versions of the propeptide were tested outside the cell in the *in vitro* assay. This suggests that these residues have little or no role in secretion recognition of the complex.

However several residues, N68, S118, Q127, D145, and T185, might have a critical role in secretion recognition. These mutant propeptides performed poorly and diminished the enzyme's extracellular activity. Some completely abolished the activity (N68 and T185) using

Fold change to Wildtype Extracellular Elastolytic Activity
0
10
20
30
40
50
60
70
80
in vivo
in vitro
R62A
L66A
P67A
N68A
R74A
Q102A
S118A
Q127A
N144A
D145A
R176A
T185A
W192A
E193A
G194A
L195A
H197A
Propeptide Residue

Figure 20. The fold change values found in Figures 17 and 19 were simplified and plotted with corresponding colors. The *in vivo* assay produced fold change values indicated by the blue bars and blue asterisks. The *in vitro* assay produced fold change values indicated by the red bars and red asterisks.

the *in vivo* assay. These substitutions still allowed the ability of the propeptide to fold and activate the mature domain but only if free from the cell and the secretion apparatus.

There were three residues, Q102, R176, and H197, which appear to have lost all ability to fold the mature domain into an active enzyme, both *in vivo* and *in vitro*. In the cell, the effects of enzyme production could not be measured using the refolding assay. This suggests these residues are intrinsically important for the ability of the enzyme to fold. These polar residues were hypothesized to form essential protein interactions at the interface of the complex.

Examining the location of these conserved residues on the model of the complex provided a rationale for how these residues were impacting the structure and stability. The residues found to be critical for secretion (N68, S118, Q127, D145, and T185) can be seen near the exterior of the complex (Figure 21). The three dimensional placement of these residues suggests they are free to interact with the secretion apparatus, thus signaling the cell that the complex is ready to be secreted.

Those mutant propeptides that diminished all ability for the enzyme to activate elastase in both the *in vivo* and the *in vitro* analysis (Q102, R176, and H197) were located on the complex model as well. All three residues were found (Figure 22) to be at the interface of the complex, potentially making protein-protein interactions with the mature domain. The H197 residue in the elastase- propeptide complex appears to be in the same location as the final histidine residue on the complex of Vibriolysin and its propeptide (Gao et al., 2010). In that case, the vibriolysin propeptide acts as an inhibitor as the C terminus of the propeptide inserts into the catalytic cleft. The carboxyl group of that final histidine actually replaces the activated water molecule in the mature enzyme. This enables the histidine residue to act as a ligand to the zinc ion. Without that water molecule in the catalytic cleft, the enzyme lacks the nucleophile to initiate peptide

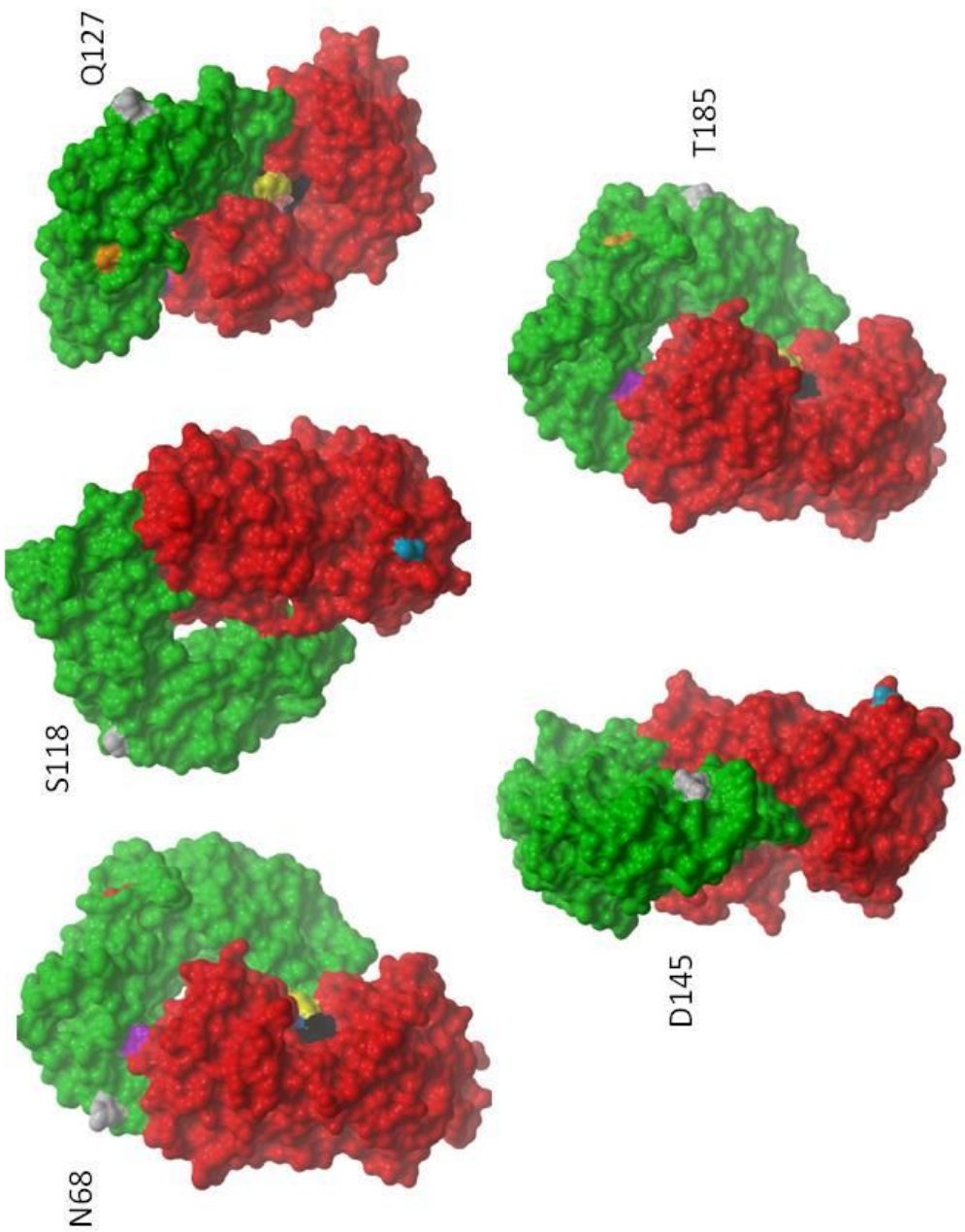
Q127
T185
S118
D145
N68

Figure 21. The critical propeptide residues implicated in secretion are N68, S118, Q127, D145, and T185. These images of the models are depicted where the mature domain is red, the propeptide is green. The active site residues of the mature domain are colored black. The amino terminal residue of the propeptide is colored orange; the carboxy terminal is yellow. The amino terminal residue of the mature domain is colored blue and the carboxy terminal residue is purple. The residues that are implicated in secretion are depicted as a grey residue in each model.

H197
R176
Q102

Figure 22. The critical propeptide residues implicated in elastase activation are Q102, R176, and H197. These images of the models are depicted where the mature domain is red, the propeptide is green. The active site residues of the mature domain are colored black. The amino terminal residue of the propeptide is colored orange; the carboxyl terminal is yellow. The amino terminal residue of the mature domain is colored blue and the carboxyl terminal residue is purple. The residues that are implicated in secretion are depicted as a grey residue in each model.

hydrolysis in addition to the propeptide physically blocking the cleft. The propeptide thus is inhibiting activity of the mature domain in the propeptide-vibriolysin complex.

In addition to those residues, there were a number of mutant propeptide residues that performed poorly in the *in vivo* assays as well as the *in vitro* assays. These residues (R62, L66, P67, N144, W192, E193, G194, and L195) could have either of the roles listed previously or could help control the propeptide stability. These models (Figure 23) provided some explanations. The R62, L66, P67, and N144 residues all appear to reside near the interface of the complex. Changing these residues to alanines diminished their ability to provide a fully functional interface for the mature domain to be activated. The residues closer to the carboxyl-terminus of the propeptide (W192, E193, G194, and L195) could be important in aiding the final histidine residue (H197) in blocking the catalytic cleft. Substituting any of these residues for an alanine could make the C-terminal tail less rigid, unable to act as an inhibitor while the mature domain folds and activates completely.

System for the production of stable propeptide-mature complexes.

These models provide a valuable tool for providing explanations for the individual residues' roles. But a clearer picture can be developed from future structure studies. To generate a complex such as the crystallized propeptide-vibriolysin complex, an inactive mature domain was needed (Figure 24). For easier purification of this complex, a Strep-Tag was employed. An allele containing the upstream region containing the *lasB* promoter, the pre signal domain, the mature domain with an E141D mutation (inactive), the Strep-Tag (EMD4Biosciences), and downstream region to allow for homologous recombination was generated using splicing by overlap-extension PCR(Horton et al., 1993; Mergulhao, Kelly, Monteiro, Taipa, & Cabral, 1999; Vallejo, Pogulis, & Pease, 2008). This allele was cloned into a suicide construct pEX18ApGW

R62
L66
P67
N144
W192
E193
G194
L195

Figure 23. The critical residues implicated in unknown yet important function are R62, L66, P67, N144, W192, E193, G194, and L195. These images of the models are depicted where the mature domain is red, the propeptide is green. The active site residues of the mature domain are colored black. The amino terminal residue of the propeptide is colored orange, the carboxy terminal is yellow. The amino terminal residue of the mature domain is colored blue and the carboxy terminal residue is purple. The residues that are implicated in secretion are depicted as a grey residue in each model.

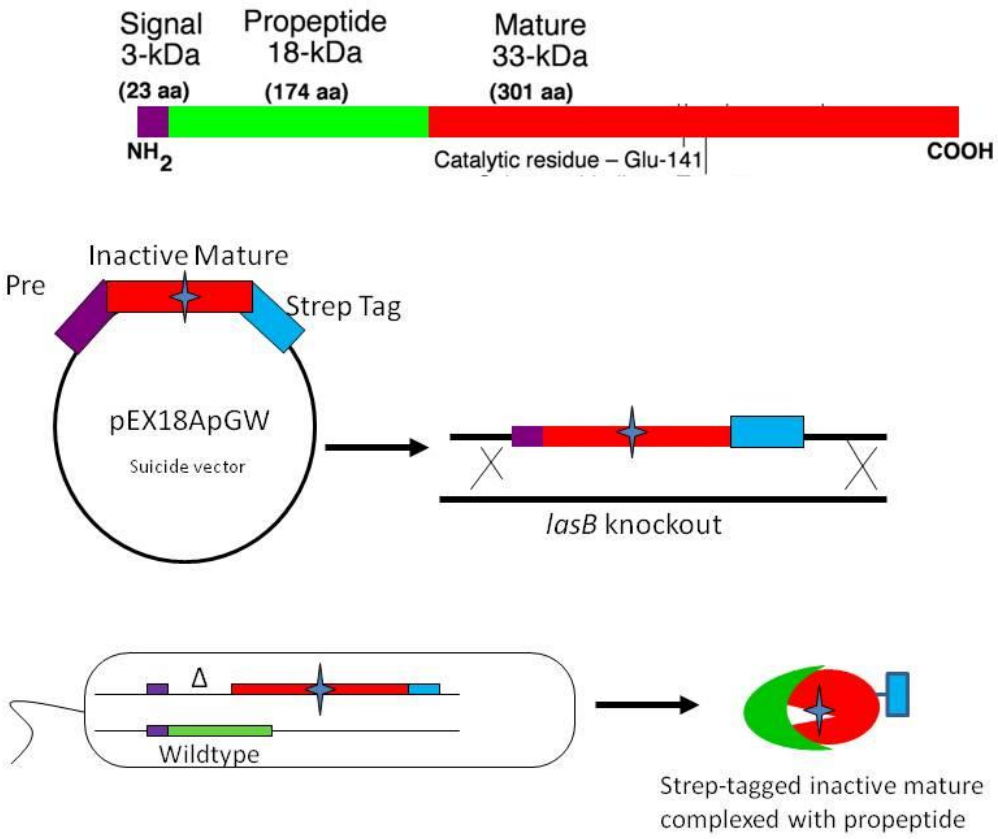
Signal
3-kDa
(23 aa)
Propeptide
18-kDa
(174 aa)
Mature
33-kDa
(301 aa)
NH2
Catalytic residue – Glu-141
COOH
Inactive Mature
Pre
Strep Tag
pEX18ApGW
Suicide vector
lasB knockout
Δ
Wildtype
Strep-tagged inactive mature
complexed with propeptide

Figure 24. A schematic of a genetic approach to produce tagged inactive propeptide-elastase complex for purification. The top illustration is the gene diagram seen in a previous figure but helps to orientate. The pre-inactive mature-strep tag construct was produced using SOEing and cloned into the suicide vector, pEX18ApGW. This suicide construct was then conjugated into a *lasB* deficient strain to cross into the host chromosome. The pre-pro allele was brought back in *trans*. The inactive mature strep-tagged domain was then capable of forming a complex with the propeptide in the periplasm.

(Choi & Schweizer, 2005) and conjugated into a *Pseudomonas* Δ*lasB* strain for homologous recombination. A vector containing the upstream regulatory region of *lasB*, the pre signal sequence and the propeptide domain was generated and conjugated into the new strain. Now the inactive tagged mature domain and the propeptide domain can fold within the periplasm to make an inactive complex for easy purification. This inactive tagged complex of mature and propeptide, where the propeptide won't be degraded, can now be used for a number of biochemical studies such as hydrogen/deuterium exchange mass spectrometry in order to determine the residues at the interface of the complex or x-ray crystallography in order to determine the entire complex's structure.

The modeling of the propeptide domain to the mature provided a visual representation to support the residue mutations and explain the data. Several of the propeptide residues when substituted were shown to be on the exterior of the complex were unable to recover the ability of the enzyme to be active in the *in vivo* assay while the activity was able to be recovered in the *in vitro* assay. Residues that showed diminished capability to aid in the mature domain's ability to activate were also shown to be localized to the interface and interior of the propeptide, providing stability to the propeptide's native structure and stability and inhibition to the mature domain. To further elucidate just how these residues at the interface interact with the mature domain, a new construct was developed to harness a tagged version of the inactive complex. Together, these results indicate there are critical residues within the propeptide that should be studied further.

SECTION 6

Summary and future directions

This dissertation contains research elucidating the ability of the propeptide of elastase, an M4 metalloprotease secreted by *Pseudomonas aeruginosa*, to act as an intramolecular chaperone through the use of several individual investigations into the structure of the propeptide and the role of individual residues (McIver et al., 1995). Each independent project resulted in new discoveries of the mechanisms required by the propeptide to aid in folding, activation and secretion of the mature domain. The following summarizes the findings from each project culminating with a discussion regarding future studies.

Previous research on similar zymogens has shown that the propeptide can act as an intramolecular chaperone for the mature domain, controlling the enzyme's activation and secretion. To elucidate just how the propeptide from elastase performs this function, a number of biochemical techniques were employed. It is currently unknown whether propeptide is capable of folding into a defined structure in order to aid mature activation within the complexed form of the two proteins. The recombinant propeptide was generated in *E. coli* to enable easier attainment than harvesting the native protein from periplasmic fractions or carefully timed, washed cellular supernatants. This recombinant propeptide allowed for milligram quantities to be purified quickly using affinity chromatography. Utilizing this purified form of recombinant propeptide, a series of circular dichroism measurements were obtained. The analysis of the signatures revealed the recombinant propeptide had a primarily beta sheet secondary structure. The purified recombinant propeptide was also subjected to a microassay-based system of crystallization screens. Further discovery of the ability of propeptide alone to form crystals in

certain crystallization cocktails supports the conclusion that the propeptide has native secondary structure. Molecular modeling techniques were then utilized to determine what this propeptide could look like. Database searches returned a crystallized structure of the propeptide-vibriolysin complex and a high degree of homology of both domains to the sequence of elastase and its propeptide. Homology modeling provided a three dimensional illustration of what the propeptide could look like based on the known propeptide structure from vibriolysin. The 3D model was analyzed based on the sequence homology and the score resulted in a 99% confidence analysis that the predicted structure is the correct structure. These investigations provided convincing evidence that the propeptide domain alone folds into a defined structure. The ability of the propeptide to have its own defined structure supports the mechanism employed by the propeptide studied extensively in the α-lytic protease activation(Anderson, Peters, Wilk, & Agard, 1999; Baker et al., 1992; Baker, Sohl et al., 1992; Bone, Frank, Kettner, & Agard, 1989; Bone, Fujishige, Kettner, & Agard, 1991; Cunningham, Jaswal, Sohl, & Agard, 1999; Cunningham, Mau, Truhlar, & Agard, 2002; Derman & Agard, 2000; Fuhrmann, Kelch, Ota, & Agard, 2004; Fujishige, Smith, Silen, & Agard, 1992; Jaswal, Sohl, Davis, & Agard, 2002; Jaswal, Truhlar, Dill, & Agard, 2005; Mace & Agard, 1995; Mace, Wilk, & Agard, 1995; Peters et al., 1998; Rader & Agard, 1997; Sauter et al., 1998; Silen et al., 1988; Silen & Agard, 1989; Silen et al., 1989; Sohl et al., 1997; Sohl et al., 1998; Truhlar & Agard, 2005). For alpha-lytic protease, the structured propeptide (“C” shaped or cup shaped) allows for the propeptide to encompass the carboxyl terminal domain of the mature domain. The mature domain is then protected to fold and activate.

In order to examine the purpose of the specific residues within the propeptide, a ClustalW alignment was performed to identify conserved residues among different propeptides within

other M4 metalloprotease sequences. This alignment produced a large number (47 residues) of conserved residues that were then individually substituted with alanine. These mutant propeptide alleles were expressed in *trans* within a *Pseudomonas* Δ*lasB* propeptide host. The mutant propeptides were synthesized by the cell and free to interact with the mature domain in the periplasm. Utilizing this system, the activity was measured outside the cell as a reflection of how the mutant propeptides were aiding the mature domain in its ability to aid in folding, activation and secretion. Each of these mutant propeptides had an effect on the ability to act as an intramolecular chaperone for the mature domain, some more than others. Certain substituted residues, such as G69, K70, E143, P177, and E187 had only a small effect on the mature domain, resulting in K_M values closer to wild-type. Other residues like N68, Q102, R176, T185, and H197 had such drastic effects on the mature domain folding and secretion that no mature was secreted and the K_M value could not be determined. Other mutant residues resulted in large changes to the K_M value, suggesting these residues are critical as well.

To examine more clearly the role of each residue, one can employ a technique to eliminate one role. This technique will negate the effect of the residue to be recognized by the secretion apparatus. The residues within the propeptide could have been contributing to the stability of the propeptide's secondary structure, sustaining interactions at the interface of the complex or being critical for the recognition of the Type 2 secretion system. The propeptide-mediated *in vitro* foldase assay utilized mutant recombinant propeptides and active enzyme. The two components were individually purified, denatured, and recombined to renature into complex form. The activity detected was then descriptive of the ability of the propeptide to act as an aid to folding and activation, not secretion. Residues were identified that had been poor in the vivo assay, but activity of the enzyme was recovered in the vitro assay (N68, S118, Q127, D145, and

T185). These residues were suggested to be essential for recognition by the secretion apparatus. A different set of residues (R62, L66, P67, R74, N144, R176, W192, E193, G194, and L195) lacked the ability to aid in folding and activation in both assays. This suggests these residues are critical for the propeptide to maintain its structure and could exist at the interface of the complex. These kinetic analyses overwhelmingly support the critical nature of these conserved residues.

Developing a three dimensional model of where these conserved residues are located, assisted in the further assessment of the residues' roles. Polar residues implicated in the role of secretion were examined and determined to be along the exterior of the complex and could easily interact with components of the secretion apparatus to signal the cell to secrete the complex. Residues implicated in folding were also examined and were found to reside along the interior of the propeptide or the interior of the complex. This suggests their critical role to stabilize the propeptide's structure and create an interface for the mature domain to attach. To further corroborate the role of these residues, a construct was developed to capture an inactive version of the complex (no degradation of the propeptide) employing a Strep-Tag. This construct could now be used for a variety of biochemical techniques to confirm the structure of the complex and the location of individual residues.

These examinations provided further supporting evidence to support the role of the propeptide as an intramolecular chaperone to the mature domain of elastase. The ability of the propeptide to have a defined native structure and conserved residues verified to be critical for the mechanism of activation and secretion, present a clearer understanding of how the propeptide is aiding in folding and providing inhibition to the activity before the complex is secreted into the medium. Future studies would address the folding and binding mechanism required of the propeptide by the mature domain.

Structural studies will confirm the residues in the complex to be exterior or interior to the complex. The crystal screens performed previously can be repeated and optimized to produce crystals large enough for diffraction. The crystals via x-ray crystallography could provide the 3D structure of the native propeptide protein to confirm the model. Furthermore the crystallized structure of the propeptide could then be docked to the crystallized structure of the mature to confirm the docked complex model. In addition purifying the inactive complex and performing crystallization screens, optimization, and diffraction, can be utilized for eventual x-ray crystallography for the determination of the whole complex structure. A quicker approach for the inactive complex could yield the residues that are at the interior of the proteins and the complex interface. Amide hydrogen/deuterium exchange mass spectrometry technology by the ExSAR Corporation would provide the residues that are buried within the complex by the difference in hydrogen/deuterium exchange rates (Yoshitomo Hamuro, Lora L. Hamuro, Stephen J. Coales, Virgil L. Woods Jr.,). Hydrogens along the exterior of the complex will exchange with the deuterium faster than those on the interior. The reaction is quenched, the complex is degraded, and mass spectrometry identifies the peptides that were deuterated. These results will provide not only the residues within the propeptide that exist at the interface, but additionally the residues within the mature domain at the interface. Mutations to mature domain would allow for assessment of their ability to recover or compensate mutant propeptide residues. This structural data would also lead to further understanding of the mechanism employed by the propeptide to be an IMC for the mature domain, i.e., what's happening within the periplasm.

An additional examination might include studying the ability of the propeptide to bind to the mature domain. If the K_M value from mutant propeptides was different from the wild-type value, this suggests the propeptide is losing the ability to bind to the mature

domain to form that complex. Differential scanning calorimetry (DSC) on the recombinant mutant propeptides compared to wild-type would determine the relative stability of these mutant propeptides, confirming those residues thought to be critical for propeptide's native structure(Sanchez-Ruiz, 2011). DSC could also be important for the assessment of mutant propeptides in complex with mature. The ability of the propeptides to be stabilizers to the complex would be reflected in this technique. Isothermal titration calorimetry could be performed on an inactive mature domain and the propeptide domain to determine the energy involved in the binding reaction (Ladbury, 2010). When two proteins bind, heat is either absorbed or generated and this thermodynamic technique measures the differences in heat to provide an assessment of the thermodynamic profile (the binding constants, enthalpy and entropy of the reaction). Optimizing these series of experiments would also eventually be useful for examination of the mutant propeptides. Moreover, this technique has its advantages compared to surface plasmon resonance (SPR), that it provides the additional thermodynamics besides the binding affinities.

Ultimately, these experiments provide a sound basis for supporting the ability of the propeptide to act as an intramolecular chaperone via its structure and roles of the conserved residues, and a goal for future research to elucidate the steps the propeptide takes to perform this function. Illuminating the way a protein proceeds from this primary amino acid sequence to its final native state is a current intense field of research, providing explanations to the structure-function relationships.

References

Adekoya, O. A., & Sylte, I. (2009). The thermolysin family (M4) of enzymes: Therapeutic and biotechnological potential. *Chemical Biology & Drug Design, 73*(1), 7-16.

Anderson, D. E., Peters, R. J., Wilk, B., & Agard, D. A. (1999). Alpha-lytic protease precursor: Characterization of a structured folding intermediate. *Biochemistry, 38*(15), 4728-4735.

Azghani, A. O., Kondepudi, A. Y., & Johnson, A. R. (1992). Interaction of pseudomonas aeruginosa with human lung fibroblasts: Role of bacterial elastase. *American Journal of Respiratory Cell and Molecular Biology, 6*(6), 652-657.

Baker, D., Silen, J. L., & Agard, D. A. (1992). Protease pro region required for folding is a potent inhibitor of the mature enzyme. *Proteins, 12*(4), 339-344.

Baker, D., Sohl, J. L., & Agard, D. A. (1992). A protein-folding reaction under kinetic control. *Nature, 356*(6366), 263-265.

Banbula, A., Potempa, J., Travis, J., Fernandez-Catalan, C., Mann, K., Huber, R., et al. (1998). Amino-acid sequence and three-dimensional structure of the staphylococcus aureus metalloproteinase at 1.72 A resolution. *Structure (London, England : 1993), 6*(9), 1185-1193.

Bever, R. A., & Iglewski, B. H. (1988). Molecular characterization and nucleotide sequence of the pseudomonas aeruginosa elastase structural gene. *Journal of Bacteriology, 170*(9), 4309-4314.

Bone, R., Frank, D., Kettner, C. A., & Agard, D. A. (1989). Structural analysis of specificity: Alpha-lytic protease complexes with analogues of reaction intermediates. *Biochemistry, 28*(19), 7600-7609.

Bone, R., Fujishige, A., Kettner, C. A., & Agard, D. A. (1991). Structural basis for broad specificity in alpha-lytic protease mutants. *Biochemistry, 30*(43), 10388-10398.

Boucher, J. C., Yu, H., Mudd, M. H., & Deretic, V. (1997). Mucoid pseudomonas aeruginosa in cystic fibrosis: Characterization of muc mutations in clinical isolates and analysis of clearance in a mouse model of respiratory infection. *Infection and Immunity, 65*(9), 3838-3846.

Bradley Brooks. (2009). ***Mariana bridi dies: Miss world finalist succumbs after amputations***. Retrieved March 13, 2011, 2011, from http://www.huffingtonpost.com/2009/01/24/mariana-bridi-dies-miss-w_n_160551.html

Braun, P., Bitter, W., & Tommassen, J. (2000). Activation of pseudomonas aeruginosa elastase in pseudomonas putida by triggering dissociation of the propeptide-enzyme complex. *Microbiology (Reading, England), 146 (Pt 10)*(Pt 10), 2565-2572.

Braun, P., Ockhuijsen, C., Eppens, E., Koster, M., Bitter, W., & Tommassen, J. (2001). Maturation of pseudomonas aeruginosa elastase. formation of the disulfide bonds. *The Journal of Biological Chemistry, 276*(28), 26030-26035.

Braun, P., Tommassen, J., & Filloux, A. (1996). Role of the propeptide in folding and secretion of elastase of pseudomonas aeruginosa. *Molecular Microbiology, 19*(2), 297-306.

Chang, C. J., Ye, J. J., Yang, C. C., Huang, P. Y., Chiang, P. C., & Lee, M. H. (2010). Influence of third-generation cephalosporin resistance on adult in-hospital mortality from post-neurosurgical bacterial meningitis. *Journal of Microbiology, Immunology, and Infection = Wei Mian Yu Gan Ran Za Zhi, 43*(4), 301-309.

Choi, K. H., & Schweizer, H. P. (2005). An improved method for rapid generation of unmarked pseudomonas aeruginosa deletion mutants. *BMC Microbiology, 5*, 30.

Conrad, J. C., Gibiansky, M. L., Jin, F., Gordon, V. D., Motto, D. A., Mathewson, M. A., et al. (2011). Flagella and pili-mediated near-surface single-cell motility mechanisms in P. aeruginosa. *Biophysical Journal, 100*(7), 1608-1616.

Cunningham, E. L., Jaswal, S. S., Sohl, J. L., & Agard, D. A. (1999). Kinetic stability as a mechanism for protease longevity. *Proceedings of the National Academy of Sciences of the United States of America, 96*(20), 11008-11014.

Cunningham, E. L., Mau, T., Truhlar, S. M., & Agard, D. A. (2002). The pro region N-terminal domain provides specific interactions required for catalysis of alpha-lytic protease folding. *Biochemistry, 41*(28), 8860-8867.

Davies, J. C., & Bilton, D. (2009). Bugs, biofilms, and resistance in cystic fibrosis. *Respiratory Care, 54*(5), 628-640.

Demidyuk, I. V., Gromova, T. Y., Polyakov, K. M., Melik-Adamyan, W. R., Kuranova, I. P., & Kostrov, S. V. (2010). Crystal structure of the protealysin precursor: Insights into propeptide function. *The Journal of Biological Chemistry, 285*(3), 2003-2013.

Derman, A. I., & Agard, D. A. (2000). Two energetically disparate folding pathways of alpha-lytic protease share a single transition state. *Nature Structural Biology, 7*(5), 394-397.

Dodero, V. I., Quirolo, Z. B., & Sequeira, M. A. (2011). Biomolecular studies by circular dichroism. *Frontiers in Bioscience : A Journal and Virtual Library, 16*, 61-73.

Dolan, M. A., Keil, M., & Baker, D. S. (2008). Comparison of composer and ORCHESTRAR. *Proteins, 72*(4), 1243-1258.

Doring, G., Maier, M., Muller, E., Bibi, Z., Tummler, B., & Kharazmi, A. (1987). Virulence factors of pseudomonas aeruginosa. *Antibiotics and Chemotherapy, 39*, 136-148.

Doring, G., Obernesser, H. J., & Botzenhart, K. (1981). Extracellular toxins of pseudomonas aeruginosa. II. effect of two proteases on human immunoglobulins IgG, IgA and secretory IgA (author's transl)]. [Extrazellulare Toxine von Pseudomonas aeruginosa. II. Einwirkung zweier gereinigter Proteasen auf die menschlichen Immunoglobuline IgG, IgA und sekretorisches IgA] *Zentralblatt Fur Bakteriologie.1.Abt.Originale.A: Medizinische Mikrobiologie, Infektionskrankheiten Und Parasitologie, 249*(1), 89-98.

Dulon, S., Leduc, D., Cottrell, G. S., D'Alayer, J., Hansen, K. K., Bunnett, N. W., et al. (2005). Pseudomonas aeruginosa elastase disables proteinase-activated receptor 2 in respiratory epithelial cells. *American Journal of Respiratory Cell and Molecular Biology, 32*(5), 411-419.

El-Bazza, Z. E., Moroz, A. F., Glatman, L. I., Samoilenko, I. I., & Terekhov, A. A. (1988). Physico-chemical and biological characteristics of pseudomonas aeruginosa elastase].

[Nekotorye fiziko-khimicheskie i biologicheskie kharakteristiki elastazy Pseudomonas aeruginosa] *Zhurnal Mikrobiologii, Epidemiologii, i Immunobiologii, (1)*(1), 3-8.

Filloux, A., Michel, G., & Bally, M. (1998). GSP-dependent protein secretion in gram-negative bacteria: The xcp system of pseudomonas aeruginosa. *FEMS Microbiology Reviews, 22*(3), 177-198.

Fuhrmann, C. N., Kelch, B. A., Ota, N., & Agard, D. A. (2004). The 0.83 A resolution crystal structure of alpha-lytic protease reveals the detailed structure of the active site and identifies a source of conformational strain. *Journal of Molecular Biology, 338*(5), 999-1013.

Fujimura, S., Nakano, Y., Takane, H., Kikuchi, T., & Watanabe, A. (2011). Risk factors for health care-associated pneumonia: Transmission of multidrug-resistant pseudomonas aeruginosa isolates from general hospitals to nursing homes. *American Journal of Infection Control, 39*(2), 173-175.

Fujishige, A., Smith, K. R., Silen, J. L., & Agard, D. A. (1992). Correct folding of alpha-lytic protease is required for its extracellular secretion from escherichia coli. *The Journal of Cell Biology, 118*(1), 33-42.

Fujita, T., Gu, Y., Kishida, N., Okinaka, K., & Ohmagari, N. (2010). Two cases of bacteremic pneumonia caused by pseudomonas aeruginosa in solid-organ cancer patients]. *Kansenshogaku Zasshi.the Journal of the Japanese Association for Infectious Diseases, 84*(5), 588-591.

Fujitani, S., Sun, H. Y., Yu, V. L., & Weingarten, J. A. (2011). Pneumonia due to pseudomonas aeruginosa: Part I: Epidemiology, clinical diagnosis, and source. *Chest, 139*(4), 909-919.

Fukushima, J., Yamamoto, S., Morihara, K., Atsumi, Y., Takeuchi, H., Kawamoto, S., et al. (1989). Structural gene and complete amino acid sequence of pseudomonas aeruginosa IFO 3455 elastase. *Journal of Bacteriology, 171*(3), 1698-1704.

Galloway, D. R. (1991). Pseudomonas aeruginosa elastase and elastolysis revisited: Recent developments. *Molecular Microbiology, 5*(10), 2315-2321.

Gao, X., Wang, J., Yu, D. Q., Bian, F., Xie, B. B., Chen, X. L., et al. (2010). Structural basis for the autoprocessing of zinc metalloproteases in the thermolysin family. *Proceedings of the National Academy of Sciences of the United States of America, 107*(41), 17569-17574.

Gray, L. D., & Kreger, A. S. (1975). Rabbit corneal damage produced by pseudomonas aeruginosa infection. *Infection and Immunity, 12*(2), 419-432.

Hay, I. D., Gatland, K., Campisano, A., Jordens, J. Z., & Rehm, B. H. (2009). Impact of alginate overproduction on attachment and biofilm architecture of a supermucoid pseudomonas aeruginosa strain. *Applied and Environmental Microbiology, 75*(18), 6022-6025.

Heck, L. W., Alarcon, P. G., Kulhavy, R. M., Morihara, K., Russell, M. W., & Mestecky, J. F. (1990). Degradation of IgA proteins by pseudomonas aeruginosa elastase. *Journal of Immunology (Baltimore, Md.: 1950), 144*(6), 2253-2257.

Heck, L. W., Morihara, K., & Abrahamson, D. R. (1986). Degradation of soluble laminin and depletion of tissue-associated basement membrane laminin by pseudomonas aeruginosa elastase and alkaline protease. *Infection and Immunity, 54*(1), 149-153.

Heck, L. W., Morihara, K., McRae, W. B., & Miller, E. J. (1986). Specific cleavage of human type III and IV collagens by pseudomonas aeruginosa elastase. *Infection and Immunity, 51*(1), 115-118.

Heiniger, R. W., Winther-Larsen, H. C., Pickles, R. J., Koomey, M., & Wolfgang, M. C. (2010). Infection of human mucosal tissue by pseudomonas aeruginosa requires sequential and mutually dependent virulence factors and a novel pilus-associated adhesin. *Cellular Microbiology, 12*(8), 1158-1173.

Hertle, R., Mrsny, R., & Fitzgerald, D. J. (2001). Dual-function vaccine for pseudomonas aeruginosa: Characterization of chimeric exotoxin A-pilin protein. *Infection and Immunity, 69*(11), 6962-6969.

Holder, I. A., & Neely, A. N. (1989). Pseudomonas elastase acts as a virulence factor in burned hosts by hageman factor-dependent activation of the host kinin cascade. *Infection and Immunity, 57*(11), 3345-3348.

Horton, R. M., Ho, S. N., Pullen, J. K., Hunt, H. D., Cai, Z., & Pease, L. R. (1993). Gene splicing by overlap extension. *Methods in Enzymology, 217*, 270-279.

Iglewski, B. H. (1996). Pseudomonas. In S. Baron (Ed.), *Medical microbiology* (4th ed.,). Galveston (TX): The University of Texas Medical Branch at Galveston.

Jacquot, J., Tournier, J. M., & Puchelle, E. (1985). *In vitro* evidence that human airway lysozyme is cleaved and inactivated by pseudomonas aeruginosa elastase and not by human leukocyte elastase. *Infection and Immunity, 47*(2), 555-560.

Jaswal, S. S., Sohl, J. L., Davis, J. H., & Agard, D. A. (2002). Energetic landscape of alpha-lytic protease optimizes longevity through kinetic stability. *Nature, 415*(6869), 343-346.

Jaswal, S. S., Truhlar, S. M., Dill, K. A., & Agard, D. A. (2005). Comprehensive analysis of protein folding activation thermodynamics reveals a universal behavior violated by kinetically stable proteases. *Journal of Molecular Biology, 347*(2), 355-366.

Jensen, P. O., Givskov, M., Bjarnsholt, T., & Moser, C. (2010). The immune system vs. pseudomonas aeruginosa biofilms. *FEMS Immunology and Medical Microbiology, 59*(3), 292-305.

Johnson, D. A., Carter-Hamm, B., & Dralle, W. M. (1982). Inactivation of human bronchial mucosal proteinase inhibitor by pseudomonas aeruginosa elastase. *The American Review of Respiratory Disease, 126*(6), 1070-1073.

Jongeneel, C. V., Bouvier, J., & Bairoch, A. (1989). A unique signature identifies a family of zinc-dependent metallopeptidases. *FEBS Letters, 242*(2), 211-214.

Kawamoto, S., Shibano, Y., Fukushima, J., Ishii, N., Morihara, K., & Okuda, K. (1993). Site-directed mutagenesis of glu-141 and his-223 in pseudomonas aeruginosa elastase: Catalytic activity, processing, and protective activity of the elastase against pseudomonas infection. *Infection and Immunity, 61*(4), 1400-1405.

Kessler, E., and D. Ohman. (2004). Pseudolysin (elastase). *The handbook of proteolytic enzymes* (2nd ed ed., pp. 401-- 409) Elsevier, Academic Press.

Kessler, E., Israel, M., Landshman, N., Chechick, A., & Blumberg, S. (1982). *In vitro* inhibition of pseudomonas aeruginosa elastase by metal-chelating peptide derivatives. *Infection and Immunity, 38*(2), 716-723.

Kessler, E., & Safrin, M. (1994). The propeptide of pseudomonas aeruginosa elastase acts an elastase inhibitor. *The Journal of Biological Chemistry, 269*(36), 22726-22731.

Kessler, E., Safrin, M., Gustin, J. K., & Ohman, D. E. (1998). Elastase and the LasA protease of pseudomonas aeruginosa are secreted with their propeptides. *The Journal of Biological Chemistry, 273*(46), 30225-30231.

Kessler, E., Safrin, M., Olson, J. C., & Ohman, D. E. (1993). Secreted LasA of pseudomonas aeruginosa is a staphylolytic protease. *The Journal of Biological Chemistry, 268*(10), 7503-7508.

Khalil, N. (1999). TGF-beta: From latent to active. *Microbes and Infection / Institut Pasteur, 1*(15), 1255-1263.

Khan, A. R., & James, M. N. (1998). Molecular mechanisms for the conversion of zymogens to active proteolytic enzymes. *Protein Science : A Publication of the Protein Society, 7*(4), 815-836.

Koh, A. Y., Mikkelsen, P. J., Smith, R. S., Coggshall, K. T., Kamei, A., Givskov, M., et al. (2010). Utility of *in vivo* transcription profiling for identifying pseudomonas aeruginosa genes needed for gastrointestinal colonization and dissemination. *PloS One, 5*(12), e15131.

Koster, M., Bitter, W., & Tommassen, J. (2000). Protein secretion mechanisms in gram-negative bacteria. *International Journal of Medical Microbiology : IJMM, 290*(4-5), 325-331.

Kou, S. C., Cherayil, B. J., Min, W., English, B. P., & Xie, X. S. (2005). Single-molecule michaelis-menten equations. *The Journal of Physical Chemistry.B, 109*(41), 19068-19081.

Ladbury, J. E. (2010). Calorimetry as a tool for understanding biomolecular interactions and an aid to drug design. *Biochemical Society Transactions, 38*(4), 888-893.

Laemmli, U. K. (1970). Cleavage of structural proteins during the assembly of the head of bacteriophage T4. *Nature, 227*(5259), 680-685.

Luft, J. R., Collins, R. J., Fehrman, N. A., Lauricella, A. M., Veatch, C. K., & DeTitta, G. T. (2003). A deliberate approach to screening for initial crystallization conditions of biological macromolecules. *Journal of Structural Biology, 142*(1), 170-179.

Lyczak, J. B., Cannon, C. L., & Pier, G. B. (2000). Establishment of pseudomonas aeruginosa infection: Lessons from a versatile opportunist. *Microbes and Infection / Institut Pasteur, 2*(9), 1051-1060.

Mabrouk, N., Deffuant, G., Tolker-Nielsen, T., & Lobry, C. (2010). Bacteria can form interconnected microcolonies when a self-excreted product reduces their surface motility:

Evidence from individual-based model simulations. *Theory in Biosciences = Theorie in Den Biowissenschaften*, *129*(1), 1-13.

Mace, J. E., & Agard, D. A. (1995). Kinetic and structural characterization of mutations of glycine 216 in alpha-lytic protease: A new target for engineering substrate specificity. *Journal of Molecular Biology*, *254*(4), 720-736.

Mace, J. E., Wilk, B. J., & Agard, D. A. (1995). Functional linkage between the active site of alpha-lytic protease and distant regions of structure: Scanning alanine mutagenesis of a surface loop affects activity and substrate specificity. *Journal of Molecular Biology*, *251*(1), 116-134.

McIver, K. S., Kessler, E., & Ohman, D. E. (2004). Identification of residues in the pseudomonas aeruginosa elastase propeptide required for chaperone and secretion activities. *Microbiology (Reading, England)*, *150*(Pt 12), 3969-3977.

McIver, K. S., Kessler, E., Olson, J. C., & Ohman, D. E. (1995). The elastase propeptide functions as an intramolecular chaperone required for elastase activity and secretion in pseudomonas aeruginosa. *Molecular Microbiology*, *18*(5), 877-889.

McIver, K. S., Olson, J. C., & Ohman, D. E. (1993). Pseudomonas aeruginosa lasB1 mutants produce an elastase, substituted at active-site his-223, that is defective in activity, processing, and secretion. *Journal of Bacteriology*, *175*(13), 4008-4015.

McKay, D. B., Thayer, M. M., Flaherty, K. M., Pley, H., & Benvegnu, D. (1992). Crystallographic structures of the elastase of pseudomonas aeruginosa. *Matrix (Stuttgart, Germany).Supplement, 1*, 112-115.

Mena, K. D., & Gerba, C. P. (2009). Risk assessment of pseudomonas aeruginosa in water. *Reviews of Environmental Contamination and Toxicology, 201*, 71-115.

Mergulhao, F. J., Kelly, A. G., Monteiro, G. A., Taipa, M. A., & Cabral, J. M. (1999). Troubleshooting in gene splicing by overlap extension: A step-wise method. *Molecular Biotechnology, 12*(3), 285-287.

Morihara, K., Tsuzuki, H., & Oda, K. (1979). Protease and elastase of pseudomonas aeruginosa: Inactivation of human plasma alpha 1-proteinase inhibitor. *Infection and Immunity, 24*(1), 188-193.

Netotea, S., Bertani, I., Steindler, L., Kerenyi, A., Venturi, V., & Pongor, S. (2009). A simple model for the early events of quorum sensing in pseudomonas aeruginosa: Modeling bacterial swarming as the movement of an "activation zone". *Biology Direct, 4*, 6.

Nickerson, N. N., Joag, V., & McGavin, M. J. (2008). Rapid autocatalytic activation of the M4 metalloprotease aureolysin is controlled by a conserved N-terminal fungalysin-thermolysin-propeptide domain. *Molecular Microbiology, 69*(6), 1530-1543.

Nirasawa, S., Nakajima, Y., Zhang, Z. Z., Yoshida, M., & Hayashi, K. (1999). Intramolecular chaperone and inhibitor activities of a propeptide from a bacterial zinc aminopeptidase. *The Biochemical Journal, 341 (Pt 1)*(Pt 1), 25-31.

Nishino, N., & Powers, J. C. (1980). Pseudomonas aeruginosa elastase. development of a new substrate, inhibitors, and an affinity ligand. *The Journal of Biological Chemistry, 255*(8), 3482-3486.

Olson, J. C., & Ohman, D. E. (1992). Efficient production and processing of elastase and LasA by pseudomonas aeruginosa require zinc and calcium ions. *Journal of Bacteriology, 174*(12), 4140-4147.

Parsek, M. R., & Greenberg, E. P. (2000). Acyl-homoserine lactone quorum sensing in gram-negative bacteria: A signaling mechanism involved in associations with higher organisms. *Proceedings of the National Academy of Sciences of the United States of America, 97*(16), 8789-8793.

Passador, L., Cook, J. M., Gambello, M. J., Rust, L., & Iglewski, B. H. (1993). Expression of pseudomonas aeruginosa virulence genes requires cell-to-cell communication. *Science (New York, N.Y.), 260*(5111), 1127-1130.

Passador, L., Tucker, K. D., Guertin, K. R., Journet, M. P., Kende, A. S., & Iglewski, B. H. (1996). Functional analysis of the pseudomonas aeruginosa autoinducer PAI. *Journal of Bacteriology, 178*(20), 5995-6000.

Pearson, J. P., Pesci, E. C., & Iglewski, B. H. (1997). Roles of pseudomonas aeruginosa las and rhl quorum-sensing systems in control of elastase and rhamnolipid biosynthesis genes. *Journal of Bacteriology, 179*(18), 5756-5767.

Peters, R. J., Shiau, A. K., Sohl, J. L., Anderson, D. E., Tang, G., Silen, J. L., et al. (1998). Pro region C-terminus:Protease active site interactions are critical in catalyzing the folding of alpha-lytic protease. *Biochemistry, 37*(35), 12058-12067.

Pitten, F. A., Panzig, B., Schroder, G., Tietze, K., & Kramer, A. (2001). Transmission of a multiresistant pseudomonas aeruginosa strain at a german university hospital. *The Journal of Hospital Infection, 47*(2), 125-130.

Pruitt, B. A.,Jr, McManus, A. T., Kim, S. H., & Goodwin, C. W. (1998). Burn wound infections: Current status. *World Journal of Surgery, 22*(2), 135-145.

Qiu, X., Kulasekara, B. R., & Lory, S. (2009). Role of horizontal gene transfer in the evolution of pseudomonas aeruginosa virulence. *Genome Dynamics, 6*, 126-139.

Rader, S. D., & Agard, D. A. (1997). Conformational substates in enzyme mechanism: The 120 K structure of alpha-lytic protease at 1.5 A resolution. *Protein Science : A Publication of the Protein Society, 6*(7), 1375-1386.

Rawlings, N. D., & Barrett, A. J. (1993). Evolutionary families of peptidases. *The Biochemical Journal, 290 (Pt 1)*(Pt 1), 205-218.

Rawlings, N. D., Barrett, A. J., & Bateman, A. (2010). MEROPS: The peptidase database. *Nucleic Acids Research, 38*(Database issue), D227-33.

Reid, T. M., & Porter, I. A. (1981). An outbreak of otitis externa in competitive swimmers due to pseudomonas aeruginosa. *The Journal of Hygiene, 86*(3), 357-362.

Reyes, M. P., Ali, A., Mendes, R. E., & Biedenbach, D. J. (2009). Resurgence of pseudomonas endocarditis in detroit, 2006-2008. *Medicine, 88*(5), 294-301.

Ritchie, D. W. (2008). Recent progress and future directions in protein-protein docking. *Current Protein & Peptide Science, 9*(1), 1-15.

Russel, M. (1998). Macromolecular assembly and secretion across the bacterial cell envelope: Type II protein secretion systems. *Journal of Molecular Biology, 279*(3), 485-499.

Rust, L., Messing, C. R., & Iglewski, B. H. (1994). Elastase assays. *Methods in Enzymology, 235*, 554-562.

Rust, L., Pesci, E. C., & Iglewski, B. H. (1996). Analysis of the pseudomonas aeruginosa elastase (lasB) regulatory region. *Journal of Bacteriology, 178*(4), 1134-1140.

Sanchez-Ruiz, J. M. (2011). Probing free-energy surfaces with differential scanning calorimetry. *Annual Review of Physical Chemistry, 62*, 231-255.

Sappington, K. J., Dandekar, A. A., Oinuma, K., & Greenberg, E. P. (2011). Reversible signal binding by the pseudomonas aeruginosa quorum-sensing signal receptor LasR. *MBio, 2*(1), 10.1128/mBio.00011-11. Print 2011.

Sauter, N. K., Mau, T., Rader, S. D., & Agard, D. A. (1998). Structure of alpha-lytic protease complexed with its pro region. *Nature Structural Biology, 5*(11), 945-950.

Schultz, D. R., & Miller, K. D. (1974). Elastase of pseudomonas aeruginosa: Inactivation of complement components and complement-derived chemotactic and phagocytic factors. *Infection and Immunity, 10*(1), 128-135.

Shanmugasundaram, N., Uma, T. S., Ramyaa Lakshmi, T. S., & Babu, M. (2009). Efficiency of controlled topical delivery of silver sulfadiazine in infected burn wounds. *Journal of Biomedical Materials Research.Part A, 89*(2), 472-482.

Shi, J., Blundell, T. L., & Mizuguchi, K. (2001). FUGUE: Sequence-structure homology recognition using environment-specific substitution tables and structure-dependent gap penalties. *Journal of Molecular Biology, 310*(1), 243-257.

Shigemura, K., Arakawa, S., Sakai, Y., Kinoshita, S., Tanaka, K., & Fujisawa, M. (2006). Complicated urinary tract infection caused by pseudomonas aeruginosa in a single institution (1999-2003). *International Journal of Urology : Official Journal of the Japanese Urological Association, 13*(5), 538-542.

Shinde, U., & Inouye, M. (1993). Intramolecular chaperones and protein folding. *Trends in Biochemical Sciences, 18*(11), 442-446.

Shinde, U., & Inouye, M. (1996). Propeptide-mediated folding in subtilisin: The intramolecular chaperone concept. *Advances in Experimental Medicine and Biology, 379*, 147-154.

Shinde, U., & Inouye, M. (2000). Intramolecular chaperones: Polypeptide extensions that modulate protein folding. *Seminars in Cell & Developmental Biology, 11*(1), 35-44.

Silen, J. L., & Agard, D. A. (1989). The alpha-lytic protease pro-region does not require a physical linkage to activate the protease domain *in vivo*. *Nature, 341*(6241), 462-464.

Silen, J. L., Frank, D., Fujishige, A., Bone, R., & Agard, D. A. (1989). Analysis of prepro-alpha-lytic protease expression in escherichia coli reveals that the pro region is required for activity. *Journal of Bacteriology, 171*(3), 1320-1325.

Silen, J. L., McGrath, C. N., Smith, K. R., & Agard, D. A. (1988). Molecular analysis of the gene encoding alpha-lytic protease: Evidence for a preproenzyme. *Gene, 69*(2), 237-244.

Silo-Suh, L. A., Elmore, B., Ohman, D. E., & Suh, S. J. (2009). Isolation, characterization, and utilization of a temperature-sensitive allele of a pseudomonas replicon. *Journal of Microbiological Methods, 78*(3), 319-324.

Sohl, J. L., Jaswal, S. S., & Agard, D. A. (1998). Unfolded conformations of alpha-lytic protease are more stable than its native state. *Nature, 395*(6704), 817-819.

Sohl, J. L., Shiau, A. K., Rader, S. D., Wilk, B. J., & Agard, D. A. (1997). Inhibition of alpha-lytic protease by pro region C-terminal steric occlusion of the active site. *Biochemistry, 36*(13), 3894-3902.

Song, Z., Wu, H., Ciofu, O., Kong, K. F., Hoiby, N., Rygaard, J., et al. (2003). Pseudomonas aeruginosa alginate is refractory to Th1 immune response and impedes host immune clearance in a mouse model of acute lung infection. *Journal of Medical Microbiology, 52*(Pt 9), 731-740.

Stark, W., Pauptit, R. A., Wilson, K. S., & Jansonius, J. N. (1992). The structure of neutral protease from bacillus cereus at 0.2-nm resolution. *European Journal of Biochemistry / FEBS, 207*(2), 781-791.

Stewart, R. M., Wiehlmann, L., Ashelford, K. E., Preston, S. J., Frimmersdorf, E., Campbell, B. J., et al. (2011). Genetic characterization indicates that a specific subpopulation of pseudomonas aeruginosa is associated with keratitis infections. *Journal of Clinical Microbiology, 49*(3), 993-1003.

Stover, C. K., Pham, X. Q., Erwin, A. L., Mizoguchi, S. D., Warrener, P., Hickey, M. J., et al. (2000). Complete genome sequence of pseudomonas aeruginosa PAO1, an opportunistic pathogen. *Nature, 406*(6799), 959-964.

Stratton, C. W. (1983). Pseudomonas aeruginosa. *Infection Control : IC, 4*(1), 36-40.

Sun, H. Y., Fujitani, S., Quintiliani, R., & Yu, V. L. (2011). Pneumonia due to pseudomonas aeruginosa: Part II: Antimicrobial resistance, pharmacodynamic concepts, and antibiotic therapy. *Chest, 139*(5), 1172-1185.

Suzuki, K., Nishiyama, Y., Sugiyama, K., Miyamoto, N., & Baba, S. (1996). Recent trends in clinical isolates from paranasal sinusitis. *Acta Oto-Laryngologica.Supplementum, 525*, 51-55.

T. Maniatis, E. F. Fritsch, J. Sambrook. (1982). *Molecular cloning: A laboratory manual*. New York: Cold Spring Harbor.

Thayer, M. M., Flaherty, K. M., & McKay, D. B. (1991). Three-dimensional structure of the elastase of pseudomonas aeruginosa at 1.5-A resolution. *The Journal of Biological Chemistry, 266*(5), 2864-2871.

Thompson, J. D., Higgins, D. G., & Gibson, T. J. (1994). CLUSTAL W: Improving the sensitivity of progressive multiple sequence alignment through sequence weighting, position-specific gap penalties and weight matrix choice. *Nucleic Acids Research, 22*(22), 4673-4680.

Tielen, P., Narten, M., Rosin, N., Biegler, I., Haddad, I., Hogardt, M., et al. (2011). Genotypic and phenotypic characterization of pseudomonas aeruginosa isolates from urinary tract infections. *International Journal of Medical Microbiology : IJMM, 301*(4), 282-292.

Tingpej, P., Smith, L., Rose, B., Zhu, H., Conibear, T., Al Nassafi, K., et al. (2007). Phenotypic characterization of clonal and nonclonal pseudomonas aeruginosa strains isolated from lungs of adults with cystic fibrosis. *Journal of Clinical Microbiology, 45*(6), 1697-1704.

Tomlin, K. L., Coll, O. P., & Ceri, H. (2001). Interspecies biofilms of pseudomonas aeruginosa and burkholderia cepacia. *Canadian Journal of Microbiology, 47*(10), 949-954.

Truhlar, S. M., & Agard, D. A. (2005). The folding landscape of an alpha-lytic protease variant reveals the role of a conserved beta-hairpin in the development of kinetic stability. *Proteins, 61*(1), 105-114.

Twining, S. S., Kirschner, S. E., Mahnke, L. A., & Frank, D. W. (1993). Effect of pseudomonas aeruginosa elastase, alkaline protease, and exotoxin A on corneal proteinases and proteins. *Investigative Ophthalmology & Visual Science, 34*(9), 2699-2712.

Vallejo, A. N., Pogulis, R. J., & Pease, L. R. (2008). PCR mutagenesis by overlap extension and gene SOE. *CSH Protocols, 2008*, pdb.prot4861.

Wiener-Kronish, J. P., & Pittet, J. F. (2011). Therapies against virulence products of staphylococcus aureus and pseudomonas aeruginosa. *Seminars in Respiratory and Critical Care Medicine, 32*(2), 228-235.

Wilder, C. N., Diggle, S. P., & Schuster, M. (2011). Cooperation and cheating in pseudomonas aeruginosa: The roles of the las, rhl and pqs quorum-sensing systems. *The ISME Journal,*

Winsor, G. L., Lam, D. K., Fleming, L., Lo, R., Whiteside, M. D., Yu, N. Y., et al. (2011). Pseudomonas genome database: Improved comparative analysis and population genomics capability for pseudomonas genomes. *Nucleic Acids Research, 39*(Database issue), D596-600.

Winsor, G. L., Van Rossum, T., Lo, R., Khaira, B., Whiteside, M. D., Hancock, R. E., et al. (2009). Pseudomonas genome database: Facilitating user-friendly, comprehensive comparisons of microbial genomes. *Nucleic Acids Research, 37*(Database issue), D483-8.

Wolynes, P. G., Onuchic, J. N., & Thirumalai, D. (1995). Navigating the folding routes. *Science (New York, N.Y.), 267*(5204), 1619-1620.

Wolz, C., Hellstern, E., Haug, M., Galloway, D. R., Vasil, M. L., & Doring, G. (1991). Pseudomonas aeruginosa LasB mutant constructed by insertional mutagenesis reveals elastolytic activity due to alkaline proteinase and the LasA fragment. *Molecular Microbiology, 5*(9), 2125-2131.

Wong, Y., Sethu, C., Louafi, F., & Hossain, P. (2011). Lipopolysaccharide regulation of toll-like receptor-4 and matrix metalloprotease-9 in human primary corneal fibroblasts. *Investigative Ophthalmology & Visual Science, 52*(5), 2796-2803.

Wretlind, B., Heden, L., Sjoberg, L., & Wadstrom, T. (1973). Production of enzymes and toxins by hospital strains of pseudomonas aeruginosa in relation to serotype and phage-typing pattern. *Journal of Medical Microbiology, 6*(1), 91-100.

Wretlind, B., & Pavlovskis, O. R. (1983). Pseudomonas aeruginosa elastase and its role in pseudomonas infections. *Reviews of Infectious Diseases, 5 Suppl 5*, S998-1004.

Xu, Z., Horwich, A. L., & Sigler, P. B. (1997). The crystal structure of the asymmetric GroEL-GroES-(ADP)7 chaperonin complex. *Nature, 388*(6644), 741-750.

Yoshitomo Hamuro, Lora L. Hamuro, Stephen J. Coales, Virgil L. Woods Jr. "Use of enhanced peptide amide Hydrogen/Deuterium exchange-mass spectrometry (DXMS) in the examination of protein-protein interactions". In Mark Chance (Ed.), *Mass spectrometry analysis for protein-protein interactions and dynamics* () Blackwell.

Yu, Y., Cheng, A. S., Wang, L., Dunne, W. M., & Bayliss, S. J. (2007). Hot tub folliculitis or hot hand-foot syndrome caused by pseudomonas aeruginosa. *Journal of the American Academy of Dermatology, 57*(4), 596-600.

Zemanick, E. T., Sagel, S. D., & Harris, J. K. (2011). The airway microbiome in cystic fibrosis and implications for treatment. *Current Opinion in Pediatrics,*

Zhang, Y. (2008). I-TASSER server for protein 3D structure prediction. *BMC Bioinformatics, 9,* 40.

APPENDICES

Table 1. pEB40 series and pEB41 of plasmids encoding for mutant propeptides.

Name of plasmid	**What it is**
pEB40	pUCP19 with EcoRI-PstI fragment of the *lasB* region including the upstream regulatory region, the pre-signal sequence, the wild-type propeptide domain and a stop codon
pEB40.D25A	pEB40 encoding a **D25A** substitution within the propeptide domain
pEB40.K59A	pEB40 encoding a **K59A** substitution within the propeptide domain
pEB40.R62A	pEB40 encoding a **R62A** substitution within the propeptide domain
pEB40.L66A	pEB40 encoding a **L66A** substitution within the propeptide domain
pEB40.P67A	pEB40 encoding a **P67A** substitution within the propeptide domain
pEB40.N68A	pEB40 encoding a **N68A** substitution within the propeptide domain
pEB40.G69A	pEB40 encoding a **G69A** substitution within the propeptide domain
pEB40.G69D	pEB40 encoding a **G69D** substitution within the propeptide domain
pEB40.K70A	pEB40 encoding a **K70A** substitution within the propeptide domain
pEB40.R74A	pEB40 encoding a **R74A** substitution within the propeptide domain
pEB40.Y75A	pEB40 encoding a **Y75A** substitution within the propeptide domain
pEB40.E76A	pEB40 encoding a **E76A** substitution within the propeptide domain
pEB40.Q77A	pEB40 encoding a **Q77A** substitution within the propeptide domain
pEB40.G81A	pEB40 encoding a **G81A** substitution within the propeptide domain
pEB40.R83A	pEB40 encoding a **R83A** substitution within the propeptide domain
pEB40.V84A	pEB40 encoding a **V84A** substitution within the propeptide domain
pEB40.V85A	pEB40 encoding a **V85A** substitution within the propeptide domain
pEB40.Q102A	pEB40 encoding a **Q102A** substitution within the propeptide domain
pEB40.G105A	pEB40 encoding a **G105A** substitution within the propeptide domain
pEB40.D114A	pEB40 encoding a **D114A** substitution within the propeptide domain
pEB40.S118A	pEB40 encoding a **S118A** substitution within the propeptide domain
pEB40.Q127A	pEB40 encoding a **Q127A** substitution within the propeptide domain
pEB40.E143A	pEB40 encoding a **E143A** substitution within the propeptide domain
pEB40.N144A	pEB40 encoding a **N144A** substitution within the propeptide domain
pEB40.D145A	pEB40 encoding a **D145A** substitution within the propeptide domain
pEB40.L149A	pEB40 encoding a **L149A** substitution within the propeptide domain
pEB40.L153A	pEB40 encoding a **L153A** substitution within the propeptide domain
pEB40.E155A	pEB40 encoding a **E155A** substitution within the propeptide domain
pEB40.L161A	pEB40 encoding a **L161A** substitution within the propeptide domain
pEB40.V162A	pEB40 encoding a **V162A** substitution within the propeptide domain
pEB40.Y163A	pEB40 encoding a **Y163A** substitution within the propeptide domain
pEB40.V165A	pEB40 encoding a **V165A** substitution within the propeptide domain
pEB40.S166A	pEB40 encoding a **S166A** substitution within the propeptide domain
pEB40.S175A	pEB40 encoding a **S175A** substitution within the propeptide domain
pEB40.R176A	pEB40 encoding a **R176A** substitution within the propeptide domain
pEB40.P177A	pEB40 encoding a **P177A** substitution within the propeptide domain
pEB40.H178A	pEB40 encoding a **H178A** substitution within the propeptide domain

pEB40.I181A	pEB40 encoding a **I181A** substitution within the propeptide domain
pEB40.D182A	pEB40 encoding a **D182A** substitution within the propeptide domain
pEB40.A813G	pEB40 encoding a **A183G** substitution within the propeptide domain
pEB40.T185A	pEB40 encoding a **T185A** substitution within the propeptide domain
pEB40.G186A	pEB40 encoding a **G186A** substitution within the propeptide domain
pEB40.E187A	pEB40 encoding a **E187A** substitution within the propeptide domain
pEB40.W192A	pEB40 encoding a **W192A** substitution within the propeptide domain
pEB40.E193A	pEB40 encoding a **E193A** substitution within the propeptide domain
pEB40.G194A	pEB40 encoding a **G194A** substitution within the propeptide domain
pEB40.L195A	pEB40 encoding a **L195A** substitution within the propeptide domain
pEB40.H197A	pEB40 encoding a **H197A** substitution within the propeptide domain
pEB41	pET28b encoding for an amino terminus Histidine-6 tag, thrombin cleavage site and propeptide domain under expression of P_{trc}
pEB41.D25A	pEB41 encoding a **D25A** substitution within the propeptide domain
pEB41.K59A	pEB41 encoding a **K59A** substitution within the propeptide domain
pEB41.R62A	pEB41 encoding a **R62A** substitution within the propeptide domain
pEB41.L66A	pEB41 encoding a **L66A** substitution within the propeptide domain
pEB41.P67A	pEB41 encoding a **P67A** substitution within the propeptide domain
pEB41.N68A	pEB41 encoding a **N68A** substitution within the propeptide domain
pEB41.G69A	pEB41 encoding a **G69A** substitution within the propeptide domain
pEB41.G69D	pEB41 encoding a **G69D** substitution within the propeptide domain
pEB41.K70A	pEB41 encoding a **K70A** substitution within the propeptide domain
pEB41.R74A	pEB41 encoding a **R74A** substitution within the propeptide domain
pEB41.Y75A	pEB41 encoding a **Y75A** substitution within the propeptide domain
pEB41.E76A	pEB41 encoding a **E76A** substitution within the propeptide domain
pEB41.Q77A	pEB41 encoding a **Q77A** substitution within the propeptide domain
pEB41.G81A	pEB41 encoding a **G81A** substitution within the propeptide domain
pEB41.R83A	pEB41 encoding a **R83A** substitution within the propeptide domain
pEB41.V84A	pEB41 encoding a **V84A** substitution within the propeptide domain
pEB41.V85A	pEB41 encoding a **V85A** substitution within the propeptide domain
pEB41.Q102A	pEB41 encoding a **Q102A** substitution within the propeptide domain
pEB41.G105A	pEB41 encoding a **G105A** substitution within the propeptide domain
pEB41.D114A	pEB41 encoding a **D114A** substitution within the propeptide domain
pEB41.S118A	pEB41 encoding a **S118A** substitution within the propeptide domain
pEB41.Q127A	pEB41 encoding a **Q127A** substitution within the propeptide domain
pEB41.E143A	pEB41 encoding a **E143A** substitution within the propeptide domain
pEB41.N144A	pEB41 encoding a **N144A** substitution within the propeptide domain
pEB41.D145A	pEB41 encoding a **D145A** substitution within the propeptide domain
pEB41.L149A	pEB41 encoding a **L149A** substitution within the propeptide domain
pEB41.L153A	pEB41 encoding a **L153A** substitution within the propeptide domain
pEB41.E155A	pEB41 encoding a **E155A** substitution within the propeptide domain
pEB41.L161A	pEB41 encoding a **L161A** substitution within the propeptide domain
pEB41.V162A	pEB41 encoding a **V162A** substitution within the propeptide domain
pEB41.Y163A	pEB41 encoding a **Y163A** substitution within the propeptide domain
pEB41.V165A	pEB41 encoding a **V165A** substitution within the propeptide domain

pEB41.S166A	pEB41 encoding a **S166A** substitution within the propeptide domain
pEB41.S175A	pEB41 encoding a **S175A** substitution within the propeptide domain
pEB41.R176A	pEB41 encoding a **R176A** substitution within the propeptide domain
pEB41.P177A	pEB41 encoding a **P177A** substitution within the propeptide domain
pEB41.H178A	pEB41 encoding a **H178A** substitution within the propeptide domain
pEB41.I181A	pEB41 encoding a **I181A** substitution within the propeptide domain
pEB41.D182A	pEB41 encoding a **D182A** substitution within the propeptide domain
pEB41.A813G	pEB41 encoding a **A183G** substitution within the propeptide domain
pEB41.T185A	pEB41 encoding a **T185A** substitution within the propeptide domain
pEB41.G186A	pEB41 encoding a **G186A** substitution within the propeptide domain
pEB41.E187A	pEB41 encoding a **E187A** substitution within the propeptide domain
pEB41.W192A	pEB41 encoding a **W192A** substitution within the propeptide domain
pEB41.E193A	pEB41 encoding a **E193A** substitution within the propeptide domain
pEB41.G194A	pEB41 encoding a **G194A** substitution within the propeptide domain
pEB41.L195A	pEB41 encoding a **L195A** substitution within the propeptide domain
pEB41.H197A	pEB41 encoding a **H197A** substitution within the propeptide domain

VITA

Personal Summary:

Emily Nicole Boice was born on the 28th of September, 1982 in Saint Louis, Missouri and is an American citizen. She graduated from Nerinx Hall High School in 2001 in Webster Groves, Missouri and went on to attend Saint Louis University from 2001-2005 where she received her Bachelors of Science degree in Biomedical Engineering.

Education:

May 2011 Ph.D. defense, Virginia Commonwealth University, Richmond, VA

Dissertation title: "The Role of the Propeptide and its Residues in Activation and Secretion of Elastase, an M4 Metalloprotease Secreted from *Pseudomonas aeruginosa*"

GPA: 3.39

Advisor: Dennis E. Ohman

May 2005 B.S. in Biomedical Engineering, Saint Louis University, Saint Louis, MO

GPA: 3.33

Awards:

- Travel Award, VCU Graduate Student Association, May 2008
- Travel Award, 12th International Pseudomonas Meeting in Hannover, Germany, August 2009
- Awarded a position in the ASM Presentation Institute, Boston, MA, May 2008
- Awarded a position in the 2008 ASM Kadner Institute, Boulder, CO, July 2008
- Awarded a position in the 2010 ASM Scientific Writing and Publishing Institute, Washington, D.C., March 2010
- Supported by the NIH Training Grant, 5T32AI007617-09, Training in Molecular Pathogenesis of Microbial Diseases

Societies:

- The Protein Society, 2010 - current

- American Association for the Advancement of Science, 2008 – current
- American Society for Microbiology, 2006 – current
- Biomedical Engineering Society, 2002 – 2005
- Engineering in Medicine and Biology Society, 2002 – 2005

Community Service:

- Student Representative of Faculty Tenure Committee, VCU, 2009
- Treasurer - Women In Science organization, 2006 – 2010
- Representative/Juror – VCU Honor Council, 2006 – 2008
- Science Museum Volunteer, 2006 – 2007

Poster Presentations:

- **Boice Emily**, E. Kessler, D. E. Ohman (August 2010) Identification of Residues in the Propeptide of *Pseudomonas* aeruginosa Elastase with Roles in its Chaperone Function. Poster presented at 24th Annual Symposium of The Protein Society in San Diego, CA.
- **Boice Emily**, E. Kessler, D. E. Ohman (August 2009) Contribution of Residues in the Propeptide of Elastase from Pseudomonas aeruginosa for Their Role in Foldase Activity. Poster presented at ASM 12th International Pseudomonas Meeting in Hannover, Germany.
- **Boice Emily,** E. Kessler, D. E. Ohman (June 2008) Characterization of the Conserved Residues in the Propeptide of *Pseudomonas aeruginosa* Elastase for Roles in Chaperone Function. Poster presented at ASM General Meeting in Boston, MA.
- **Boice Emily**, D. E. Ohman. (May 2008) Techniques Utilized in the Characterization of the Intramolecular Chaperone of *Pseudomonas aeruginosa* Elastase. John C. Forbes Graduate Students Honors Colloquim Presentation at MCV in Richmond, VA.
- **Boice Emily**, D. E. Ohman (April 2008). Molecular Models of the Propeptide-Elastase Complex to Aid in Examination of the Interface and Identification of Critical Residues. VCU Annual Graduate Student Research Symposium & Exhibit. Poster presented at VCU in Richmond, VA.
- **Boice Emily**, D. E. Ohman. (March 2008). Critical Residues Identified for Elastolytic Activity of Elastase Secreted by *P. aeruginosa*. William and Mary Graduate Student

Association Symposium. Poster presented at College of William and Mary in Williamsburg, VA.

- **Boice Emily**, E. Kessler, D. E. Ohman. (August 2007). *In vitro* Renaturation of An Active Elastase By Its Intramolecular Chaperone. Poster presented at ASM 11th International Pseudomonas Conference in Seattle, WA.
